



ESA-MOST Dragon Cooperation

中国科技部-欧洲空间局“龙计划”合作

2017 DRAGON 4 SYMPOSIUM

2017年“龙计划”四期学术研讨会

**Terrain Correction Methods for Multi-Dimensional SAR
Data Applied to Forest AGB Estimation**

Erxue Chen¹, Zengyuan Li¹, Lei Zhao¹,

Wen Hong², Laurent Ferro Famil³

¹ Institute of Forest Resources Information Technique, CAF

²Institute of Electronic , CAS

26-30 June 2017 | Copenhagen, Denmark

2017年6月26-30日, 丹麦 哥本哈根

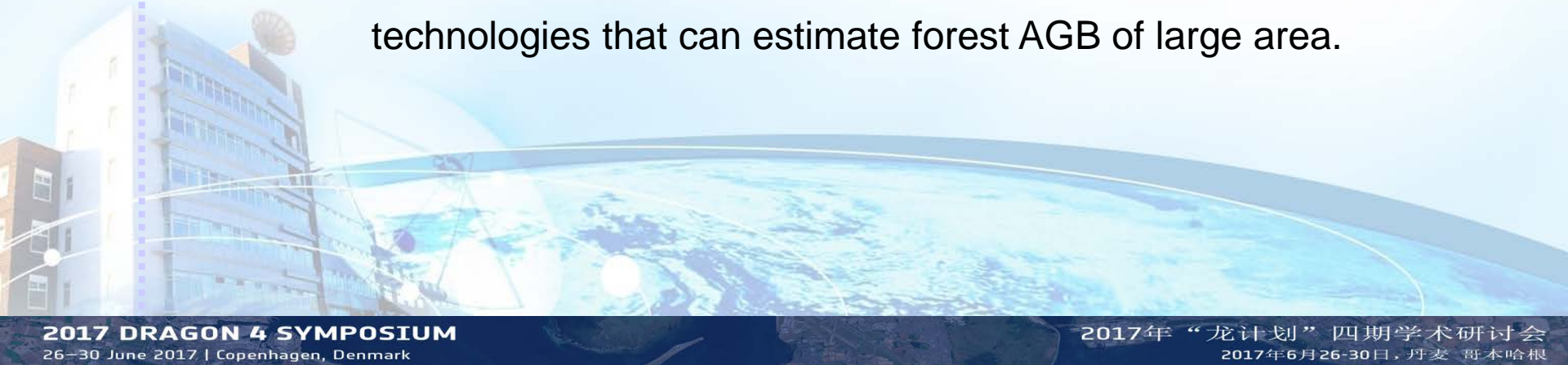
³I.E.T.R - Univ Rennes 1

1. Background
2. Three-Stage Terrain Correction Method For PolSAR
3. Terrain Correction Method For InSAR coherence
4. The combined estimation approach of Forest AGB
based on CASMSAR (X-InSAR, P-PoSAR)
5. Summary

1. Background
2. Three-Stage Terrain Correction Method For PolSAR
3. Terrain Correction Method For InSAR coherence
4. The combined estimation approach of Forest AGB
based on CASMSAR (X-InSAR, P-PoSAR)
5. Summary

1. Background

- Single-Dimensional SAR
 - Single-Polarization; Single-Frequency; Single-Baseline.
- Multi-Dimensional SAR (Yirong Wu, 2013)
 - Multi-Polarization; Muti-Frequency; Multi-Baseline; and their Combinations.
- Based on Multi-Dimensional SAR, we can obtain more characteristics associated with forest AGB.
 - Multi-Dimensional SAR is one of the most promising technologies that can estimate forest AGB of large area.



1. Background

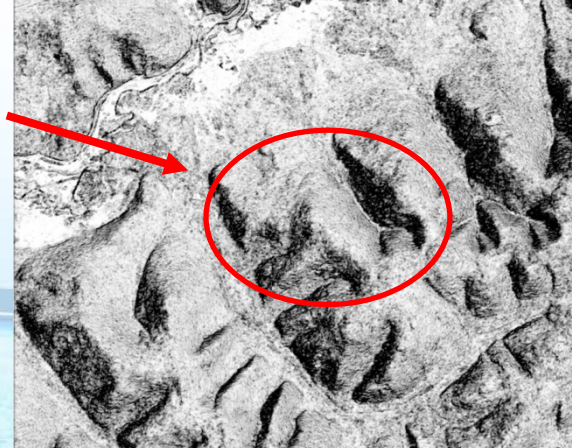
- Terrain effects is a big problem for the application of Single/Multi-Dimensional SAR data
 - Owing to the characteristics of side-looking illumination by SAR sensors.
- Current terrain correction methods are not fully applicable to Multi-Dimensional SAR data
 - Most methods proposed for a single backscatter intensity value

→ Radar illumination



PolSAR PauliRGB

→ Radar illumination



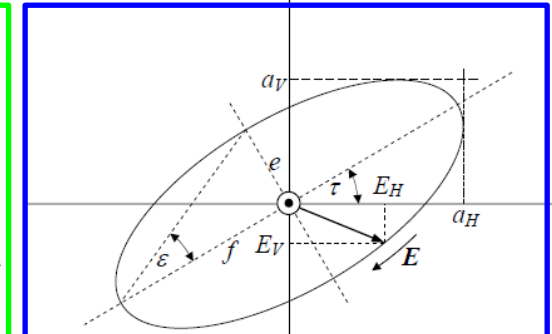
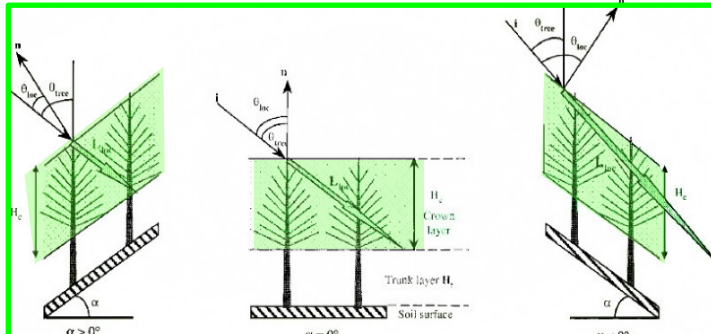
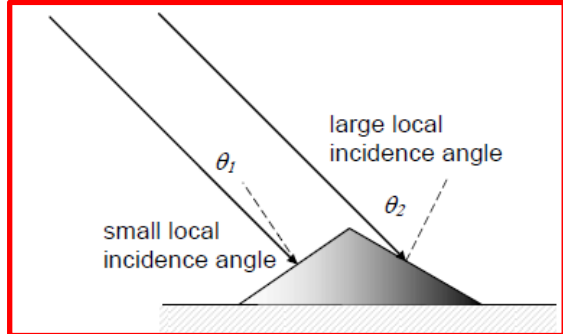
InSAR Coherence

Outlines

1. Background
2. Three-Stage Terrain Correction Method for PolSAR
3. Terrain Correction Method for InSAR coherence
4. The combined estimation approach of forest AGB
based on CASMSAR (X-InSAR, P-PoSAR)
5. Summary

2.1 Background

- The influence of topography on PolSAR image
 - Variation of **Effective Scattering Area (ESA)**
 - It is due to radar observation geometry and local terrain. In other words, it is the variation of the number of the scatterer in one pixel.
 - Variation of local scattering mechanisms, etc.
 - This phenomenon is commonly known as **Angular Variation Effect (AVE)** that mainly appears in vegetation area
 - Variation of polarization states
 - It is caused by azimuth slopes that induce **Polarization Orientation Angle (POA)** changes.



2.1 Background

- Effective Scattering Area correction (ESAc)

- Based on local incidence angle

$$\sigma^0 = \beta^0 \cdot \sin \theta_{loc} \quad (\text{Freeman, 1989})$$

- Based on surface tilt angles

$$\sigma^0 = \beta^0 \cdot \sin(\theta - \theta_r) \cos \theta_a \quad (\text{Zyl, 1993})$$

- Based on projection angle

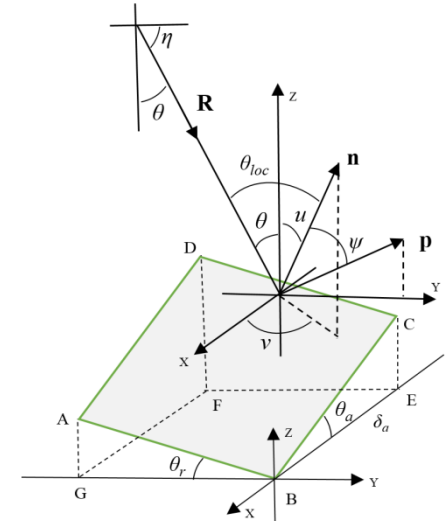
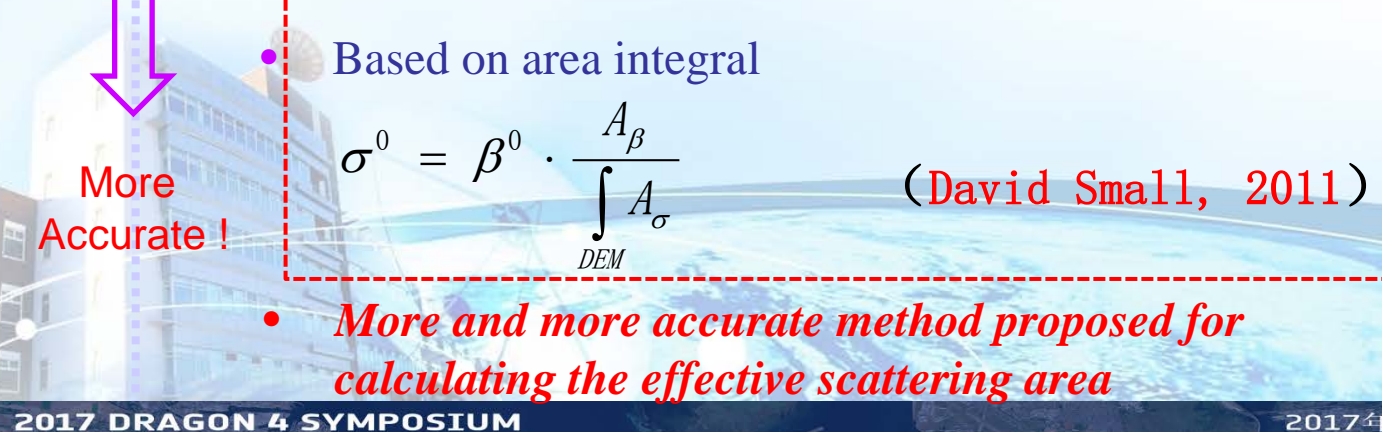
$$\sigma^0 = \beta^0 \cdot \cos \psi \quad (\text{Ulander, 1996})$$

- Based on area integral

$$\sigma^0 = \beta^0 \cdot \frac{\int A_\sigma}{\int A_\beta} \quad (\text{David Small, 2011})$$

- *More and more accurate method proposed for calculating the effective scattering area*

More
Accurate !



2.1 Background

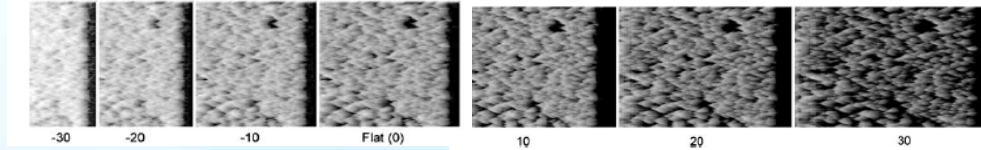
- Angular Variation Effect correction (AVEc)

Basic Model: $\sigma_{\theta_{loc}} \approx \sigma / \cos^n(\theta_{loc})$ ***n is the core !!!***

- Based on semi-empirical model derived from radiative transfer model

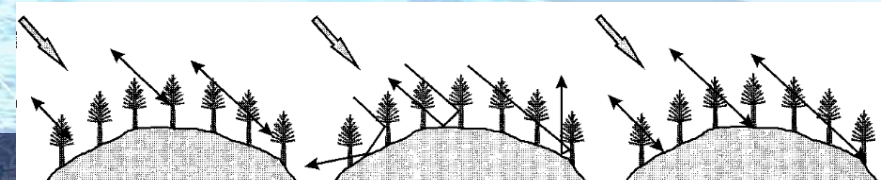
$$n = 1 + a \log \left(\frac{1 - \exp(-b\tau)}{1 - \exp(-c\tau)} \right) \quad \tau: \text{crown optical depth} \quad (\text{T. Castel, 2001})$$

- Based simulate SAR image derived from forward simulate model



(G. Sun, 2002)

- These method can not adaptively determining the value of n and not suitable to PolSAR matrix data.***



2.1 Background

- Polarization Orientation Angle correction (POAc)
 - Based on Local imaging geometry (DEM) (Lee; Schuler, 2000)

$$\tan \theta_p = \frac{\tan \theta_a}{-\tan \theta_r \tan \theta + \sin \theta} \quad \theta_p \text{ POA shift angle}$$

- Based circular polarization method

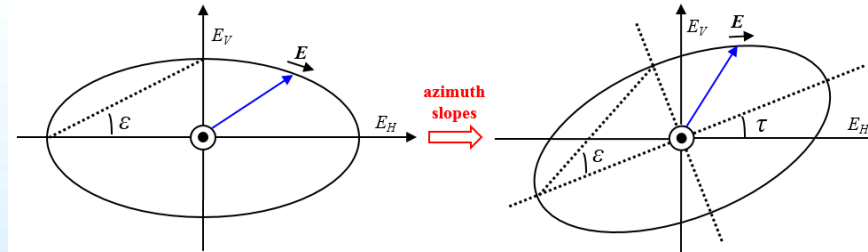
$$\theta_p = \operatorname{Arg}(\langle S_{RR} S_{LL}^* \rangle) / 4$$

S_{RR} : right-right circular polarization
 S_{LL} : left-left circular polarization

The most
commonly used
algorithms!

$$C = \begin{bmatrix} \langle |S_{HH}|^2 \rangle & \langle \sqrt{2}S_{HH}S_{HV}^* \rangle & \langle S_{HH}S_{VV}^* \rangle \\ \langle \sqrt{2}S_{HV}S_{HH}^* \rangle & \langle 2|S_{HV}|^2 \rangle & \langle \sqrt{2}S_{HV}S_{VV}^* \rangle \\ \langle S_{VV}S_{HH}^* \rangle & \langle \sqrt{2}S_{WW}S_{HV}^* \rangle & \langle |S_{WW}|^2 \rangle \end{bmatrix}$$

$$C_{POAC} = VCV^T$$



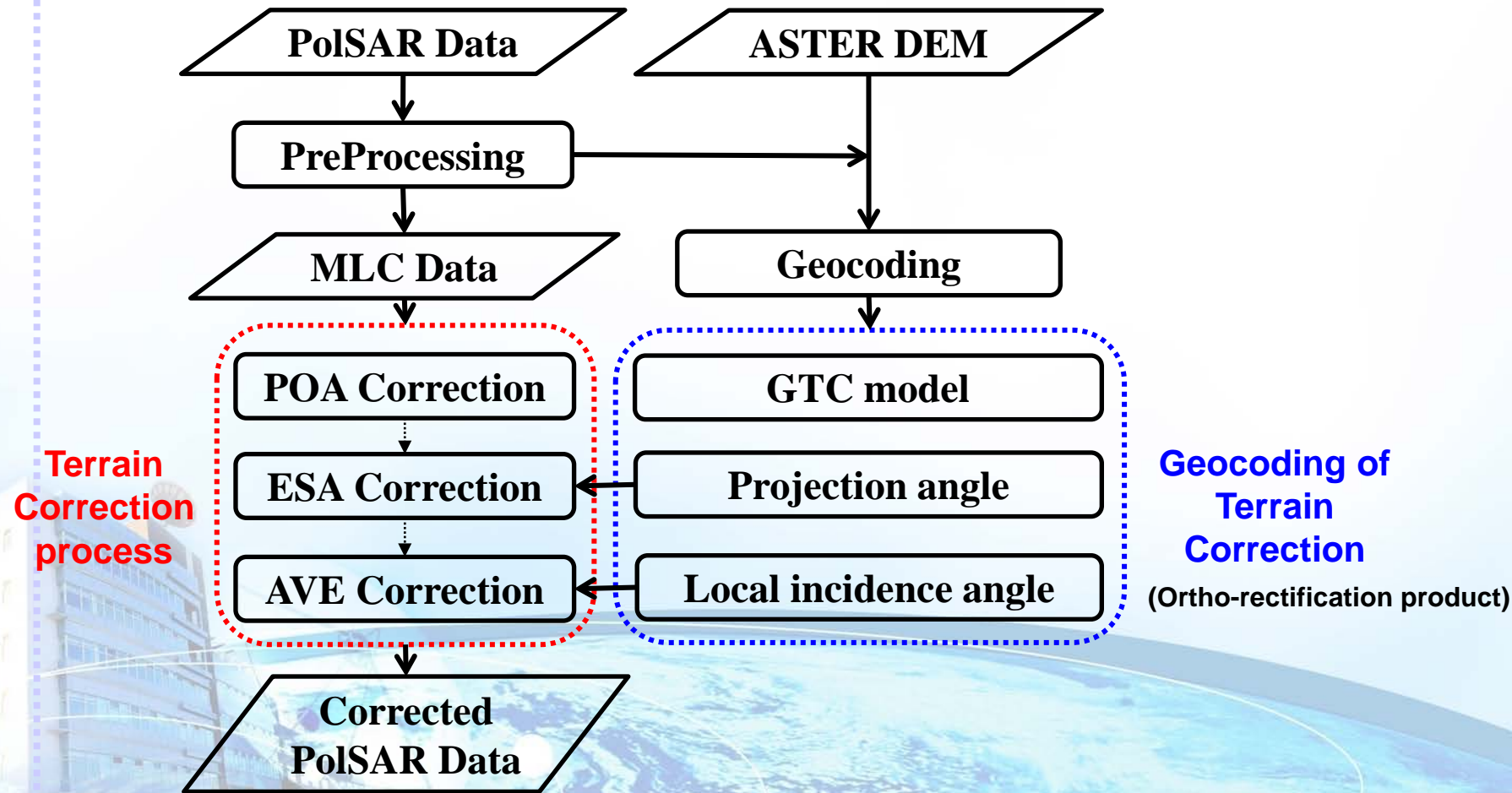
τ : polarization orientation angle

ε : ellipticity angle

$$V = \frac{1}{2} \begin{bmatrix} 1 + \cos 2\theta & \sqrt{2} \sin 2\theta & 1 - \cos 2\theta \\ -\sqrt{2} \sin 2\theta & 2 \cos 2\theta & \sqrt{2} \sin 2\theta \\ 1 - \cos 2\theta & -\sqrt{2} \sin 2\theta & 1 + \cos 2\theta \end{bmatrix}$$

2.2 Methods

- Flow chart



2.2 Methods

- Three-Stage Terrain Correction

$$\sigma_{rtc}^0 = \boxed{\sigma_{POC}^0} \cdot \boxed{\cos \psi} \cdot \boxed{\left(\frac{\cos \theta_{ref}}{\cos \theta_{loc}} \right)^n}$$

$$C_{POC} = VCV^T$$

$$V = \frac{1}{2} \begin{bmatrix} 1 + \cos 2\theta & \sqrt{2} \sin 2\theta & 1 - \cos 2\theta \\ -\sqrt{2} \sin 2\theta & 2 \cos 2\theta & \sqrt{2} \sin 2\theta \\ 1 - \cos 2\theta & -\sqrt{2} \sin 2\theta & 1 + \cos 2\theta \end{bmatrix}$$

Stage①:POA Correction

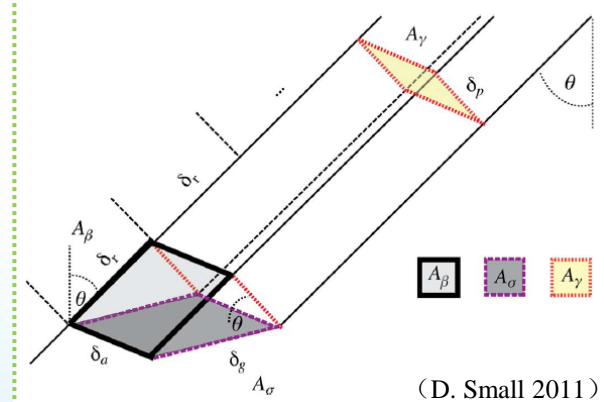
- Circular polarization method

Stage②:ESA Correction

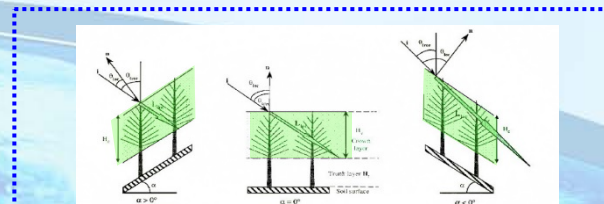
- Projection angle method

Stage③:AVE Correction

- Minimum correlation coefficient method



(D. Small 2011)



2017年“龙计划”四期学术研讨会
2017年6月26-30日，丹麦，哥本哈根

2.2 Methods

- Minimum correlation coefficient method
 - We can evaluate the correction result by the correlation between corrected backscatter value and the local incident angle.

$$\sigma_{\theta_{loc}} = \sigma \cdot \left(\frac{\cos \theta_{ref}}{\cos \theta_{loc}} \right)^n \quad \Leftrightarrow \quad f(n) = \rho(\theta_{loc}, \sigma_{\theta_{loc}})$$

$$n = \arg \min \{abs[f(n)]\}$$

- The value of **n** for each polarization channel: $n(hh)=N_1, n(hv)=N_2, n(vv)=N_3$
- So, we get the correction coefficient for each polarization channel :

$$k_{hh} = \left(\frac{\cos \theta_{ref}}{\cos \theta_{loc}} \right)^{N_1} \quad k_{hv} = \left(\frac{\cos \theta_{ref}}{\cos \theta_{loc}} \right)^{N_2} \quad k_{vv} = \left(\frac{\cos \theta_{ref}}{\cos \theta_{loc}} \right)^{N_3}$$

- Finally, the correction coefficient matrix **K** for polarization covariance matrix **C** is:

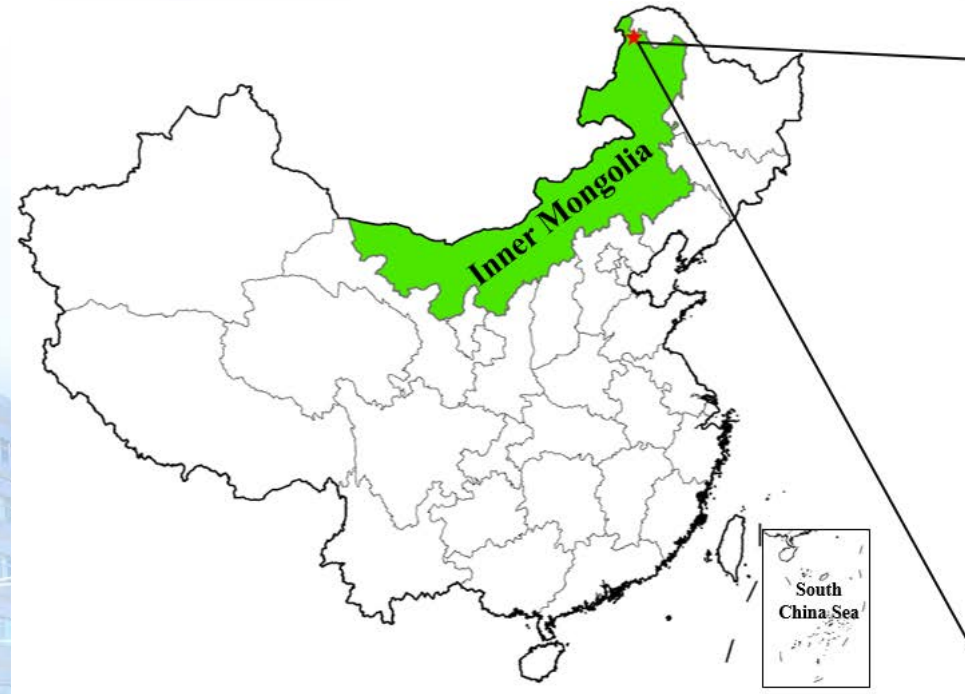
$$K = \begin{bmatrix} k_{hh} & \sqrt{k_{hh}k_{hv}} & \sqrt{k_{hh}k_{vv}} \\ \sqrt{k_{hh}k_{hv}} & k_{hv} & \sqrt{k_{hv}k_{vv}} \\ \sqrt{k_{hh}k_{vv}} & \sqrt{k_{hv}k_{vv}} & k_{vv} \end{bmatrix}$$

$$C_{out} = C \odot K$$

Note: \odot is the Hadamard product.

2.3 Test Data

- DaXingAnLing test site in Inner Mongolia
 - The location of study site:

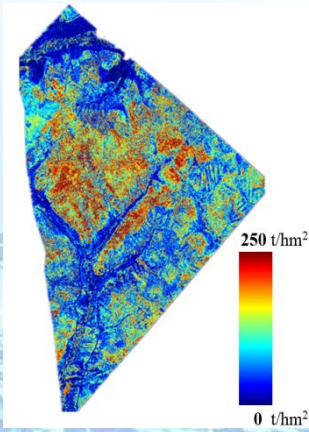
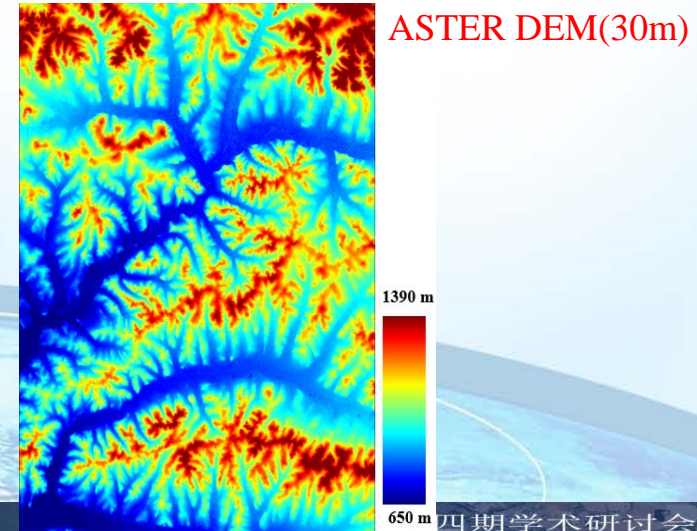
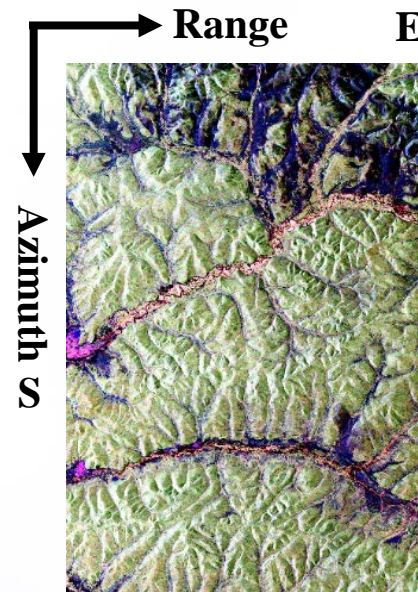


 ALOS2 PALSAR2
 LiDAR forest AGB



2.3 Test Data

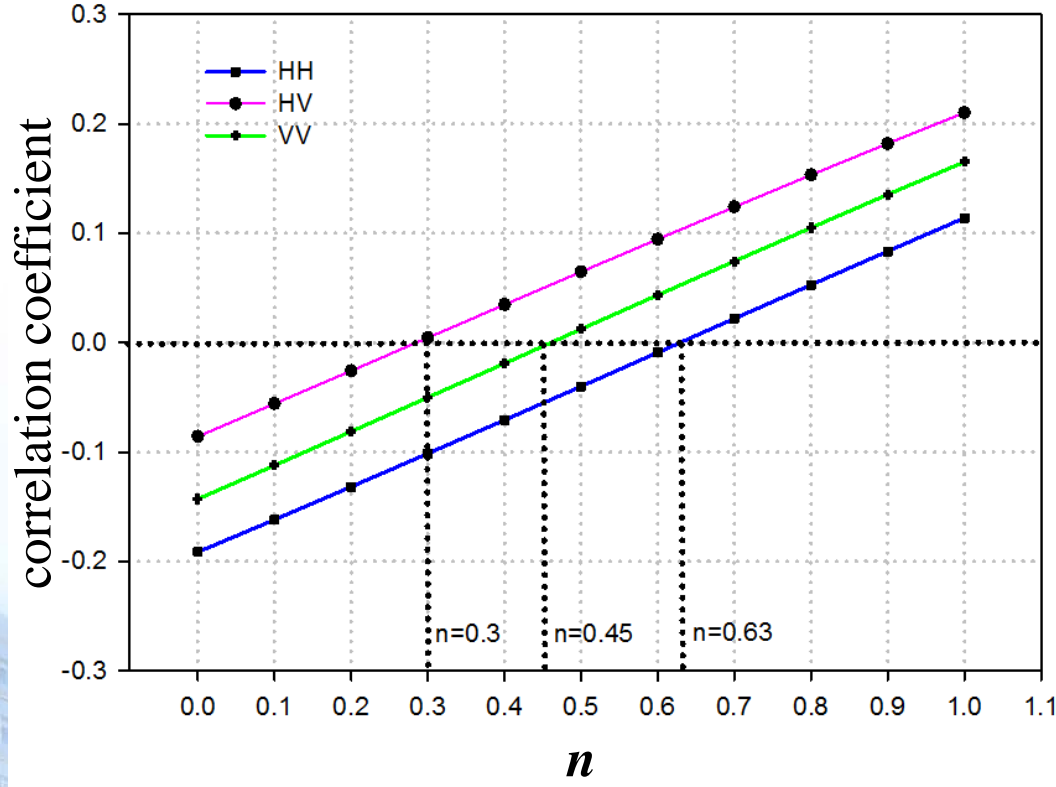
- Data
 - PolSAR Data
 - ALOS-2 PALSAR-2 HBQ
 - 2014-8-29
 - L-band
 - $2.64 \text{ m} \times 2.86\text{m}$
 - Reference Data



2.4 Result and Analysis

- Angular Variation Effect correction (AVEc)

- Minimum correlation coefficient method



$$f(n) = \rho(\theta_{loc}, \sigma_{\theta_{loc}})$$

$$n = \arg \min \{abs[f(n)]\}$$

$n(hh)=0.63$

$n(hv)=0.30$

$n(vv)=0.45$



$$K = \begin{bmatrix} m^{0.630} & m^{0.465} & m^{0.540} \\ m^{0.465} & m^{0.300} & m^{0.375} \\ m^{0.540} & m^{0.375} & m^{0.450} \end{bmatrix}$$

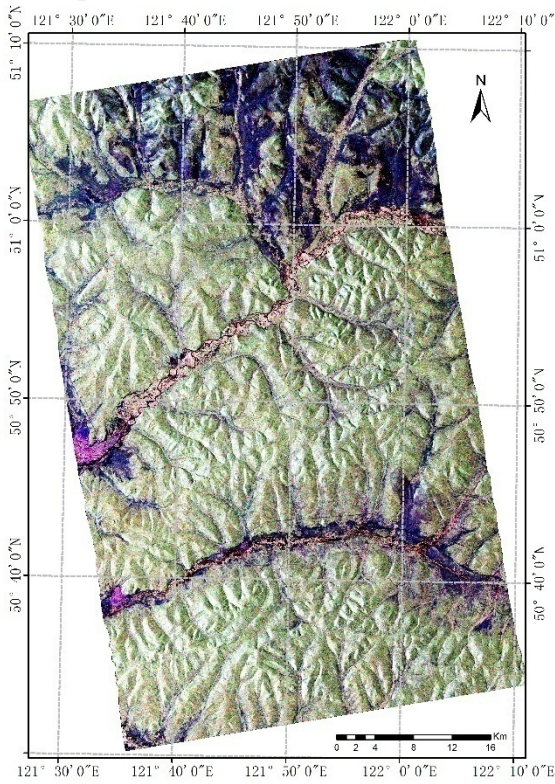
$$m = \frac{\cos \theta_{ref}}{\cos \theta_{loc}}$$

$$C_{out} = C \odot K$$

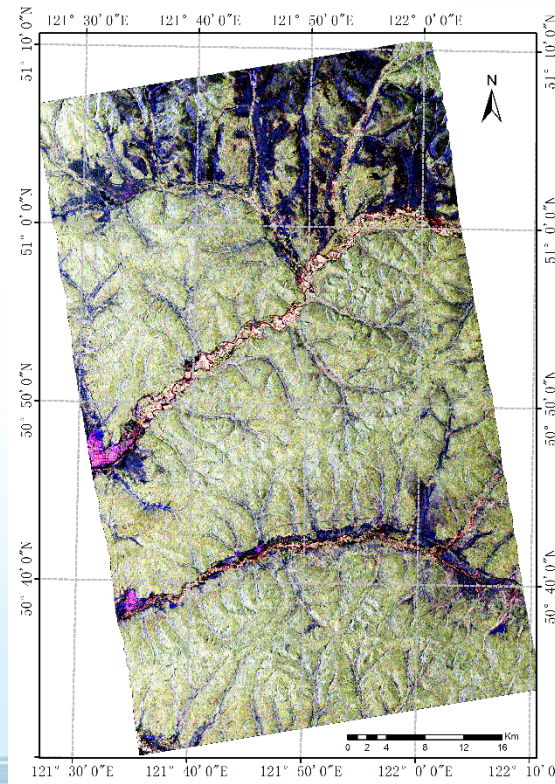
- The same values of n corresponding to different correlations coefficient. This illustrates that different polarization should adopt different values of n.

2.4 Result and Analysis

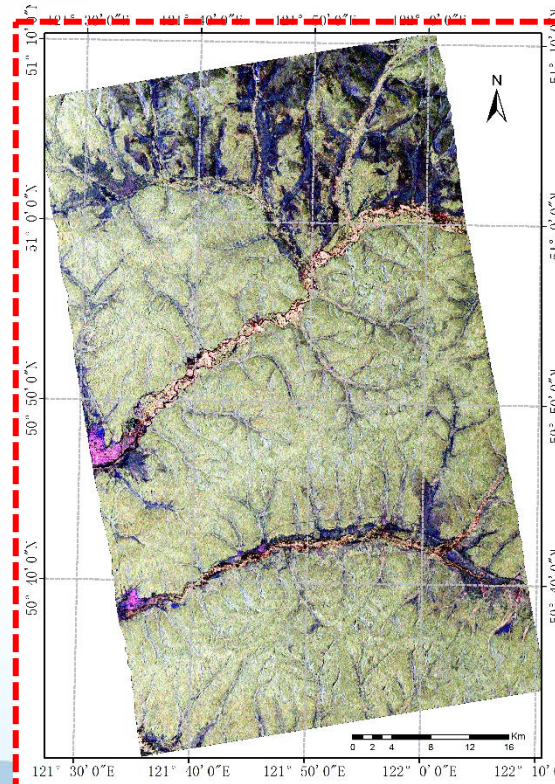
- Angular Variation Effect correction result (AVEc)



GTC Pauli RGB



POAc+ESAc Pauli RGB

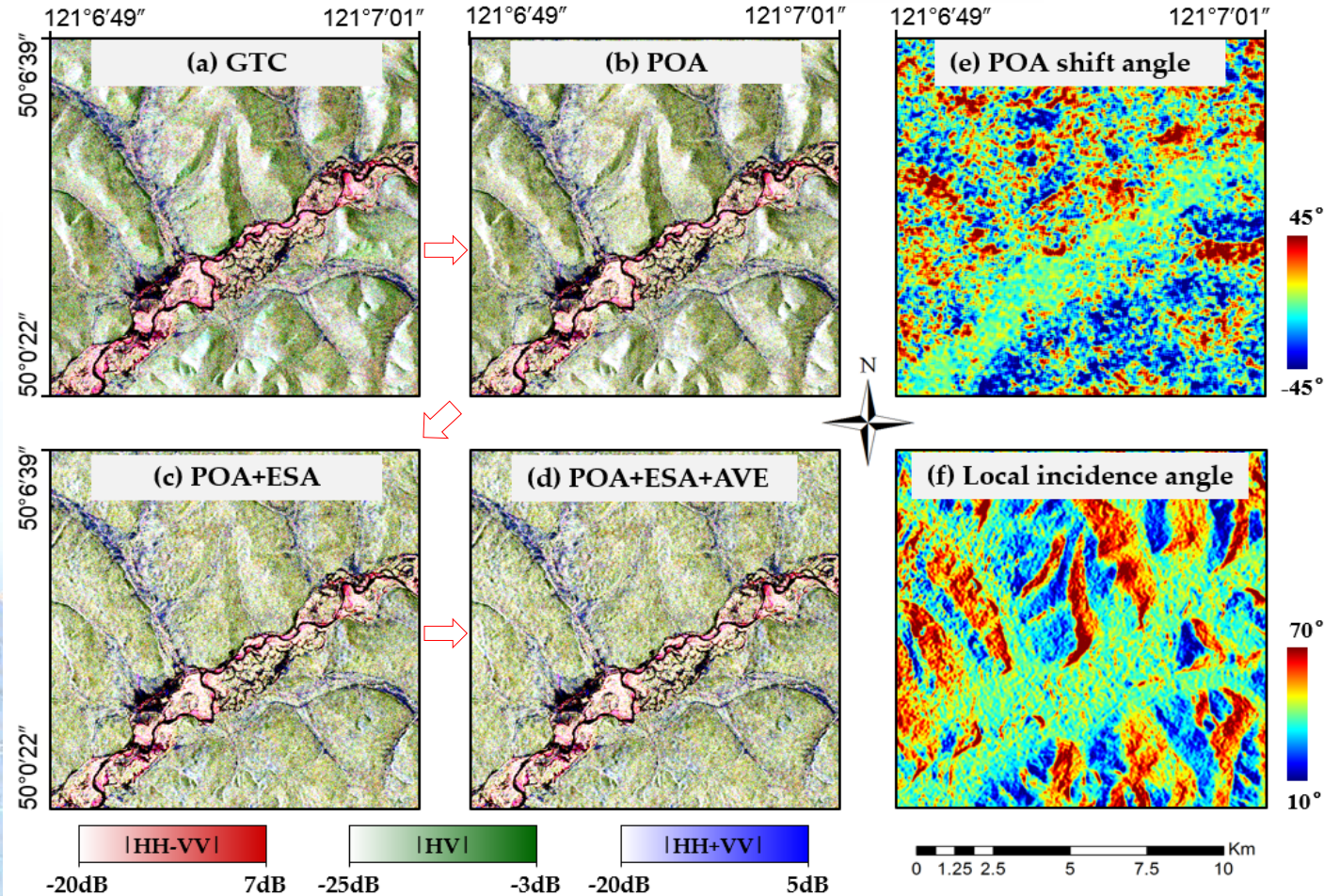


POAc+ESAc+AVEc Pauli RGB

- The remaining terrain effects in PolSAR image has been effectively removed, there is no significant difference between front slope and back slope.*

2.4 Result and Analysis

- Different stage Terrain Correction result (Enlarged)

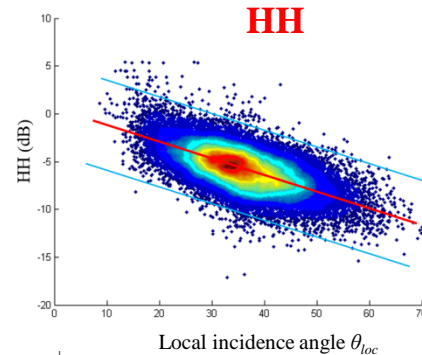


2.4 Result and Analysis

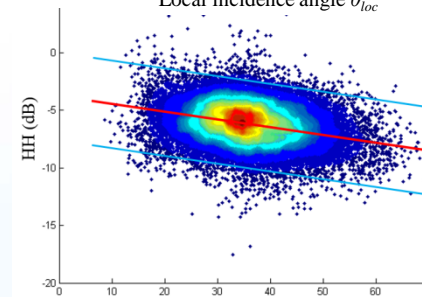


- Terrain Correction results of different stage

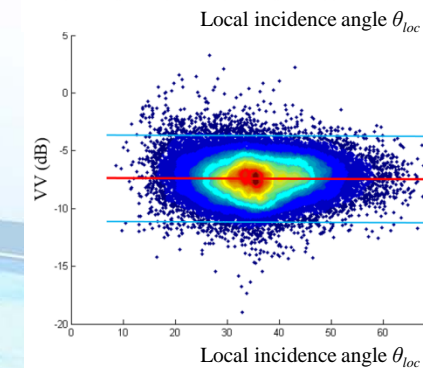
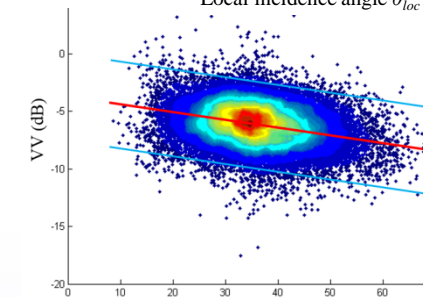
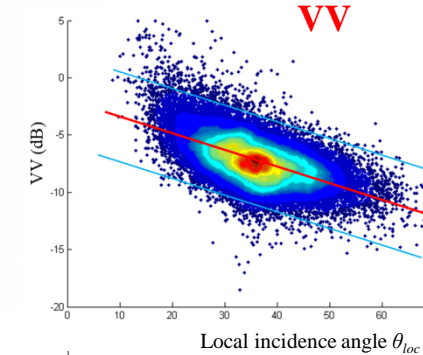
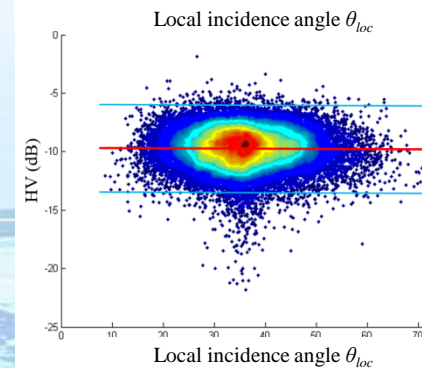
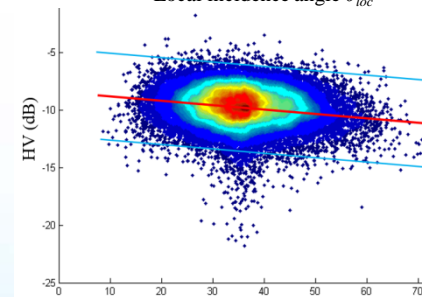
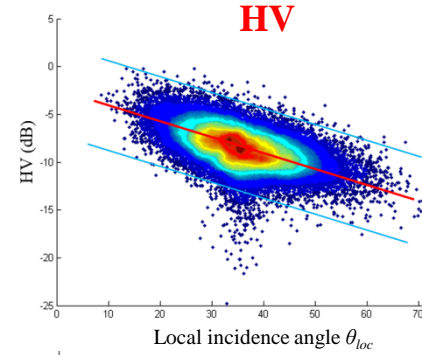
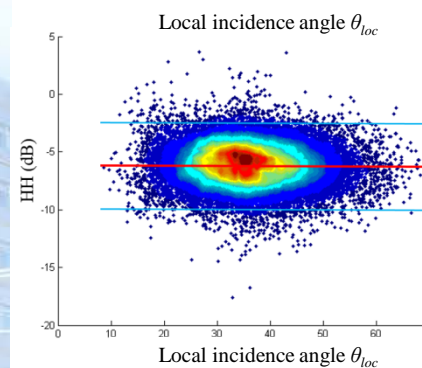
GTC



POAc
+
ESAc



POAc
+
ESAc
+
AVEc

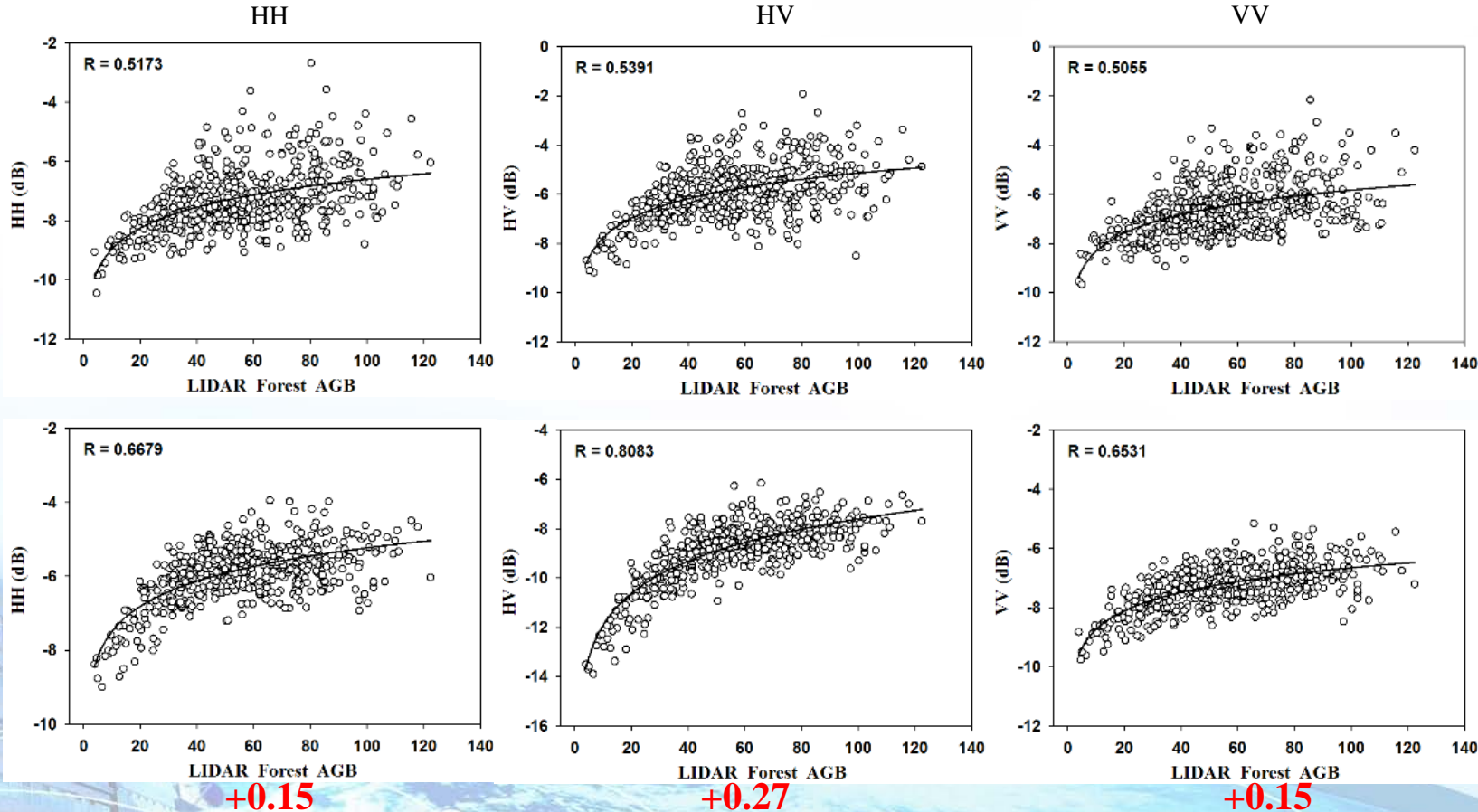


Compare scatter plots of different correction stage, along with the correction stages performed, the correction result is getting better and better.

2.4 Result and Analysis

- The correlation between backscatter coefficient and forest AGB

Before
correction

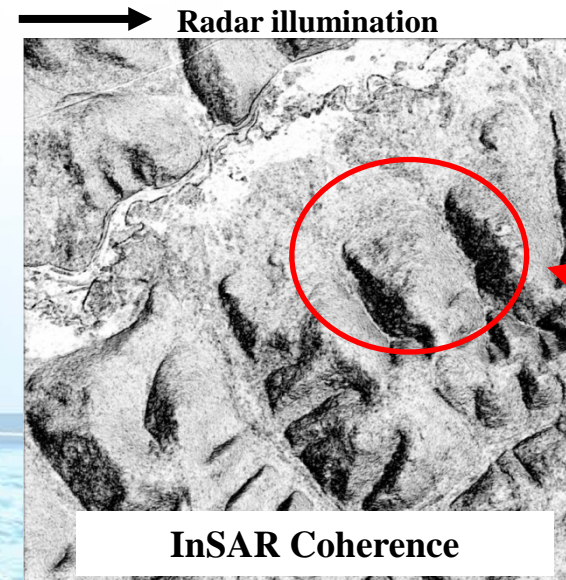


- Obviously, the corrected backscatter coefficients have the better correlation with forest AGB than uncorrected case.

1. Background
2. Three-Stage Terrain Correction Method For PolSAR
3. Terrain Correction Method For InSAR coherence
4. The combined estimation approach of Forest AGB
based on CASMSAR (X-InSAR, P-PoSAR)
5. Summary

3.1 Background

- InSAR coherence is an important feature for land cover type mapping and forest AGB estimation.
- InSAR coherence is also affected by terrain relief.
- There are few correction method developed for forest applications.
- We developed **SINC** differential correction method for InSAR coherence.

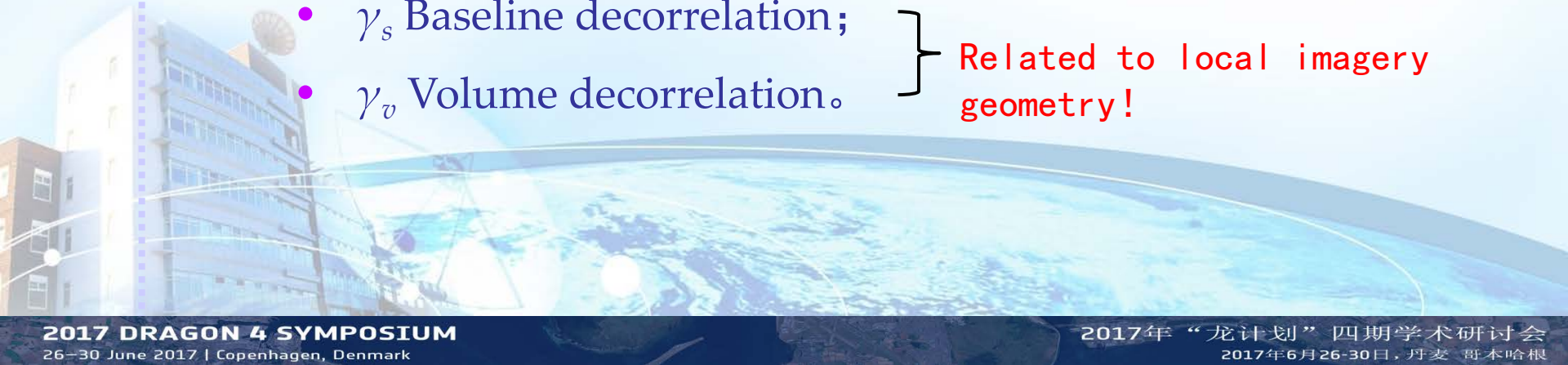


3.2 Methods

- Sources of InSAR decorrelation (Coherence)

$$\gamma = \gamma_{SNR} \cdot \gamma_t \cdot \gamma_{proc} \cdot \gamma_s \cdot \gamma_v \quad (\text{Cloude, 2009})$$

- γ_{SNR} Signal-to-noise decorrelation;
 - γ_t Temporal decorrelation;
 - γ_{proc} Data processing decorrelation;
 - γ_s Baseline decorrelation;
 - γ_v Volume decorrelation.
- } Related to local imagery geometry!



3.2 Methods

- Baseline decorrelation

$$\gamma_s = 1 - \frac{cB_{\perp}}{W\lambda R \tan(\theta - \eta)}$$

(Cloude, 2009; Yongsheng Zhou, 2010)

- c : Speed of light;
 - B_{\perp} : Vertical baseline;
 - λ : Wave length;
 - η : Slope angle;
 - θ : Radar look angle.
 - W : Bandwidth;
 - R : Slant-range.
- ***Baseline decorrelation can be compensated by above model.***



3.2 Methods

- Volume decorrelation

$$\gamma_v = \frac{\int_0^h f(h) e^{jk_z h} dh}{\int_0^h f(h) dh} \quad k_z = \frac{2\pi B_{\perp}}{\lambda R \sin \theta}$$

(Cloude, 2009; Yongsheng Zhou, 2010)

- SINC model (while $f(h)$ is a constant):

$$\gamma_v = \frac{\sin(k_z h / 2)}{k_z h / 2} = \text{sinc}(k_z h / 2)$$

- Based on the relationship between K_z and slope angle(η), the relationship between γ_v and η is established:

$$k_z^{\text{slope}} = \frac{2\pi B_{\perp}}{\lambda R \sin(\theta - \eta)} \quad \rightarrow \quad \gamma_v = \text{sinc} \left[\frac{h\pi B_{\perp}}{\lambda R \sin(\theta - \eta)} \right]$$

3.2 Methods

- Volume decorrelation

$$\gamma_v = \text{sinc} \left[\frac{h\pi B_{\perp}}{\lambda R \sin(\theta - \eta)} \right]$$

Forest-dependent parameter (FDP)

Forest height (h)

Forest-independent parameter (FIP)

Vertical baseline (B_{\perp}) ; Wave length (λ) ;

Look angle (θ) ; Slope angle (η) ;

Slant-range (R)

- The **purpose** of coherence terrain correction :

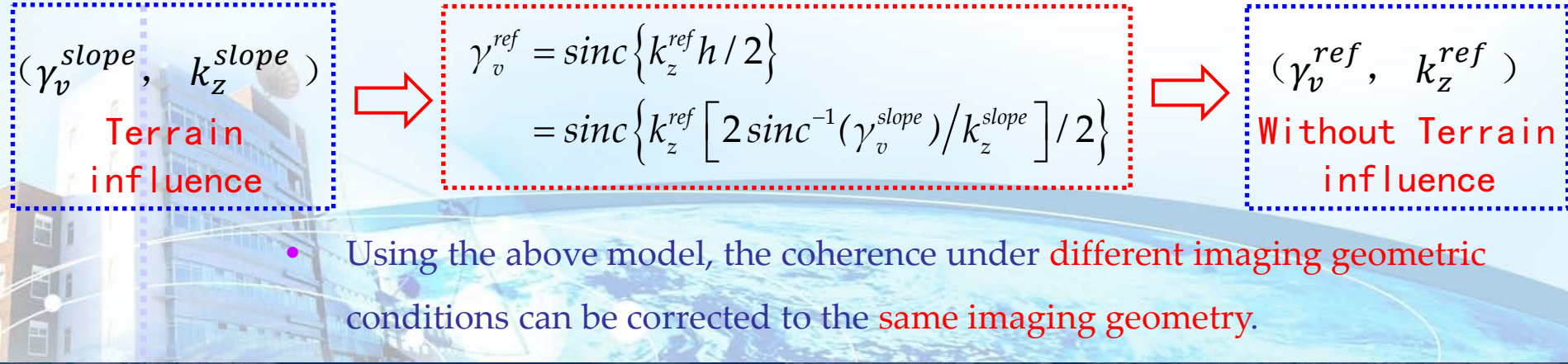
- Removal the effect of FIP on coherence;
- Only preserves the effect of FDP on coherence.

3.2 Methods

- The derivation of differential coherence model
 - The volume decorrelation model considering the terrain effect:

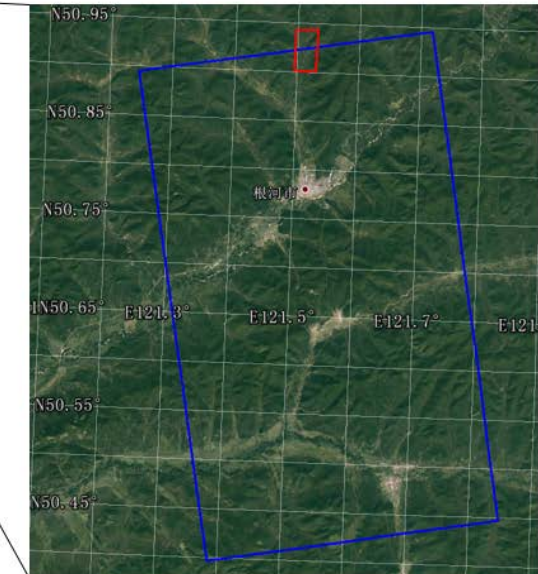
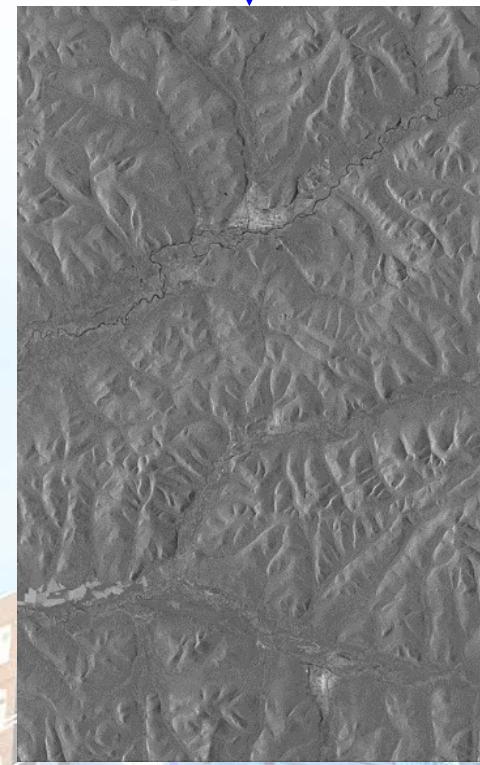
$$\text{Model 1: } \gamma_v^{\text{slope}} = \text{sinc}(k_z^{\text{slope}} h / 2)$$
 - The volume decorrelation model without considering the terrain effect:

$$\text{Model 2: } \gamma_v^{\text{ref}} = \text{sinc}(k_z^{\text{ref}} h / 2)$$
 - From the model 1 to solve the FDP parameter, then substituted into the model 2. The **difference equation of coherence** was derived as follows:



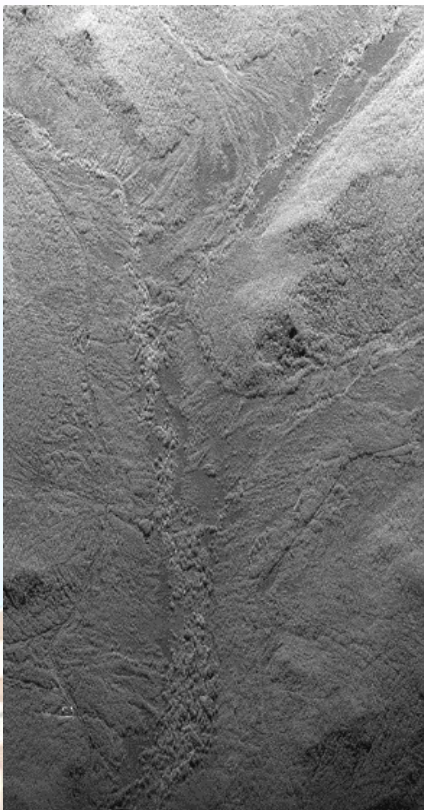
3.3 Test Data

- DaXingAnLing test site in Inner Mongolia
 - Space borne TanDEM-X InSAR data
 - Airborne double antenna X-band InSAR data



3.3 Test Data

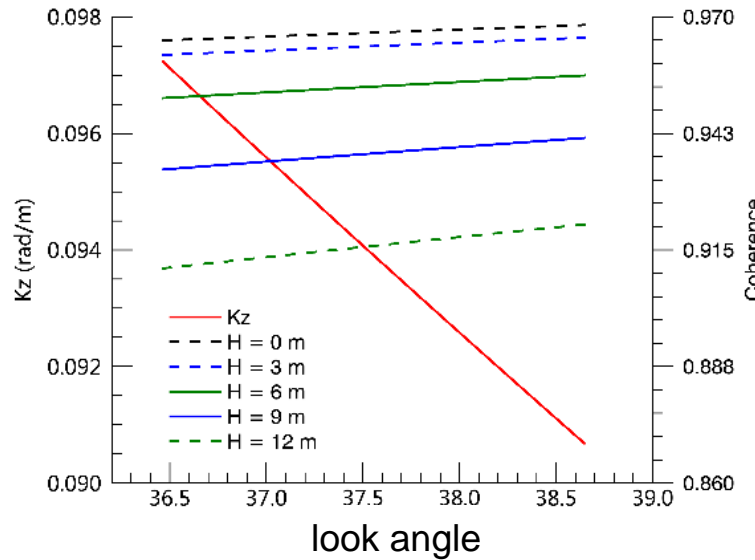
- DaXingAnLing test site in Inner Mongolia
 - Space borne TanDEM-X InSAR data 
 - Airborne double antenna X-band InSAR data 



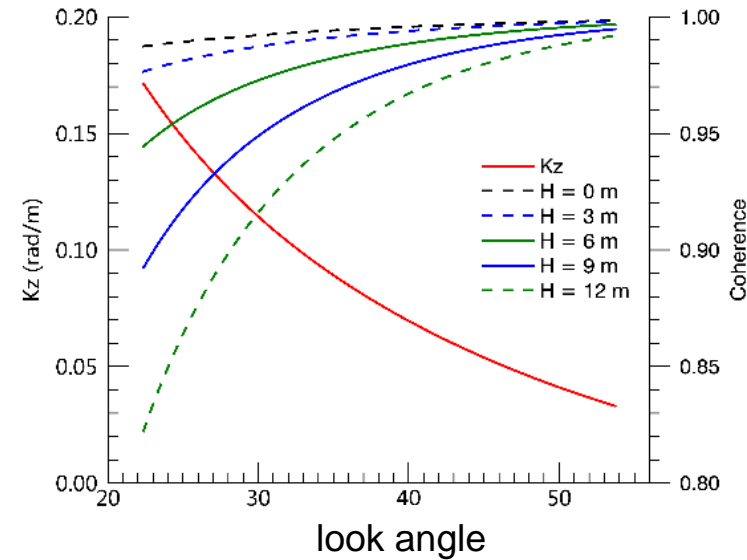
| InSAR data parameter | | |
|-----------------------|---------------------|-------------------|
| Data parameter | SAR sensors | |
| | TanDEM/TerraSAR-X | CASMSAR-X |
| Date of imaging | 2012.8.14 | 2013.09.13 |
| polarization mode | HH | HH |
| Range resolution (m) | 1.36 | 0.25 |
| Azimuth Resolution(m) | 2.02 | 0.34 |
| Platform height(km) | 515.6 | 5.8 |
| flight direction | From south to north | From west to east |
| Lookangle range | 36.5° - 38.6° | 22° - 54° |
| Bandwidth(MHz) | 100 | 600 |
| Baseline(m) | 216 | 2.2 |

3.4 Result and Analysis

- The coherence simulation analysis based on space borne and airborne InSAR parameters
 - Influence of Radar look angle on coherence under flat terrain.



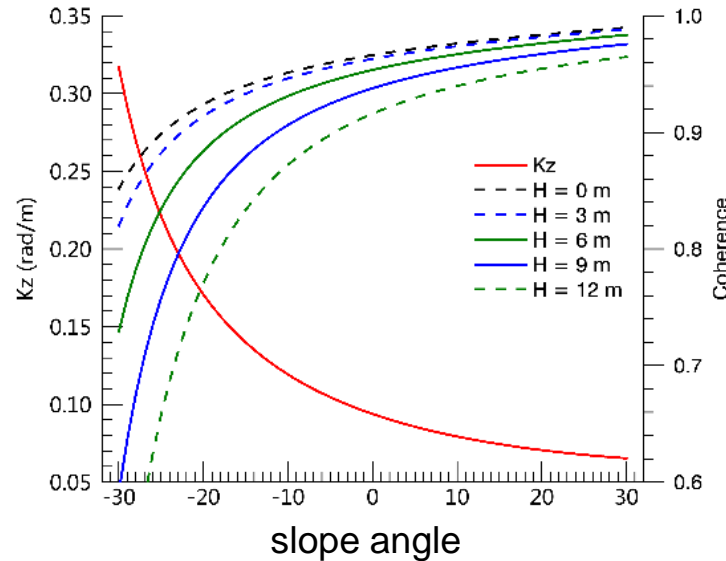
TanDEM/TerraSAR
Small look angle range



CASMSAR-X
Big look angle range

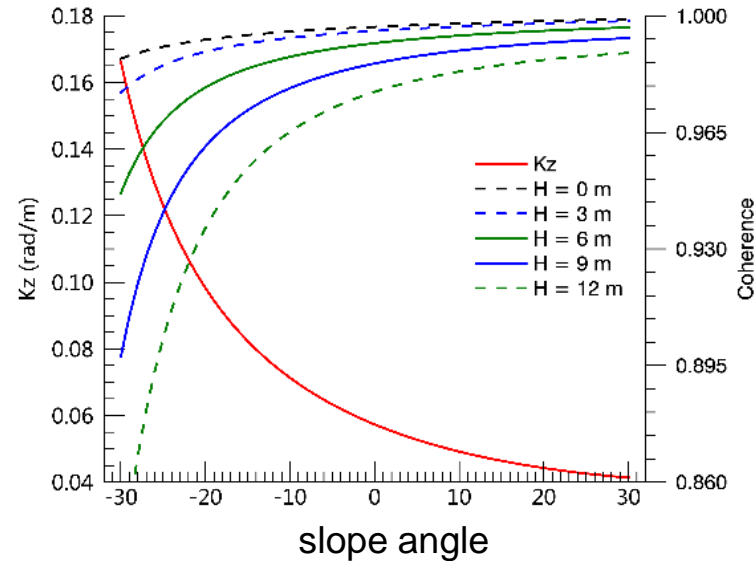
3.4 Result and Analysis

- The coherence simulation analysis based on space borne and airborne InSAR parameters
 - Influence of slope angle on coherence under Fixed look angle (Center look angle)



TanDEM-X InSAR

- The coherence of TanDEM-X is more affected by the slope angle.*

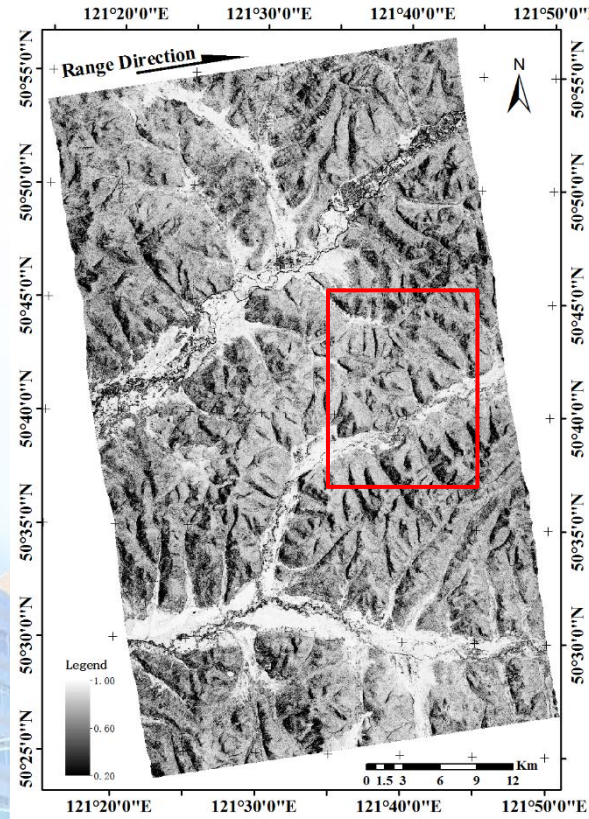


CASMSAR-X

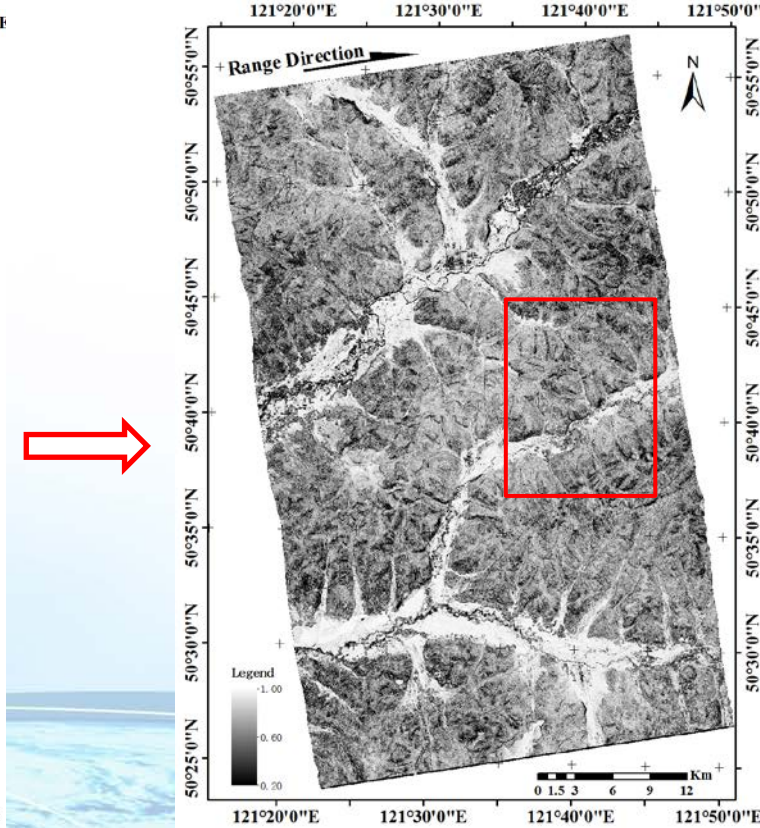
3.4 Result and Analysis

- The coherence correction results of space borne InSAR

Range direction

Before correction

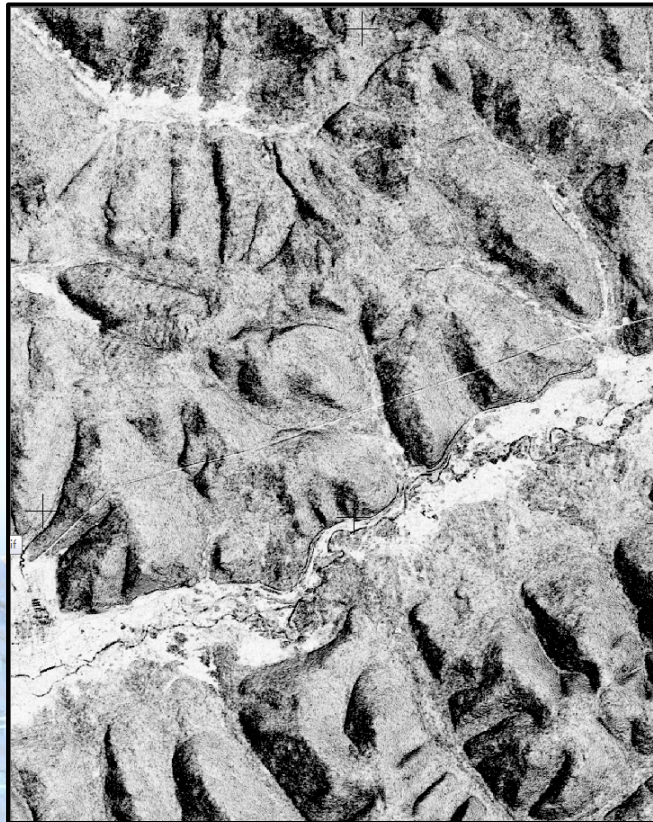


After correction

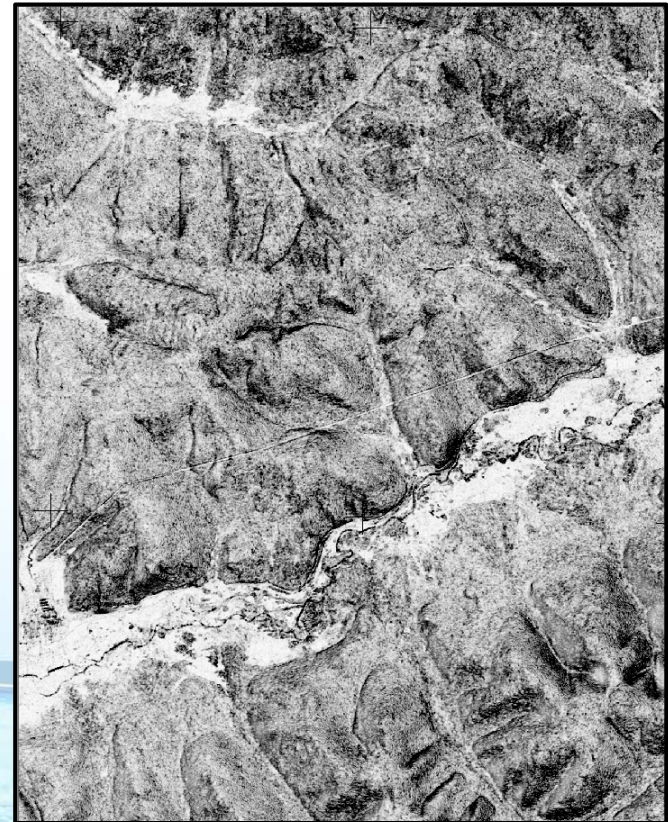
3.4 Result and Analysis

- The coherence correction results of **space borne InSAR**
(Enlarged)

Range
direction
→



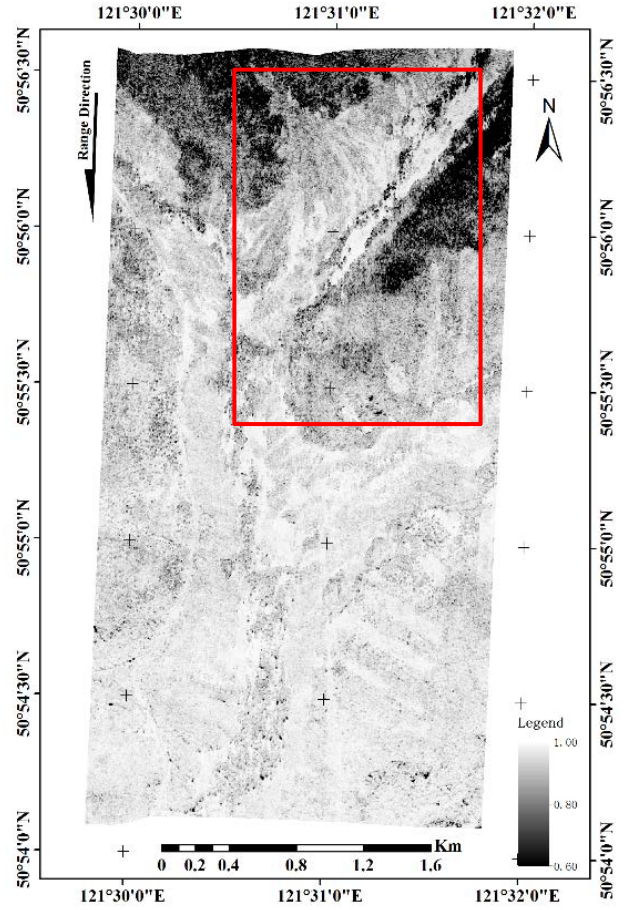
Before correction



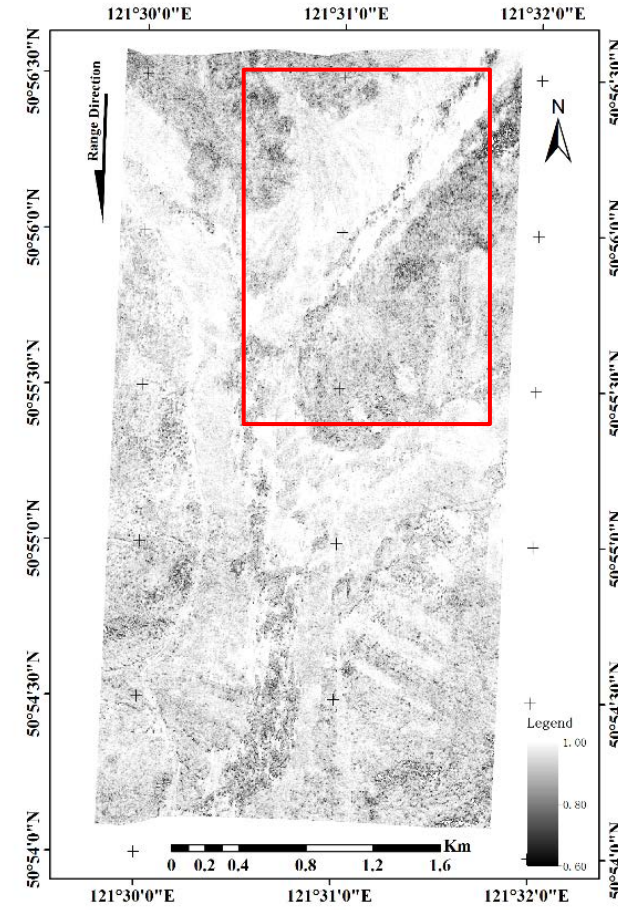
After correction

3.4 Result and Analysis

- The coherence correction results of Airborne InSAR



Before correction



After correction

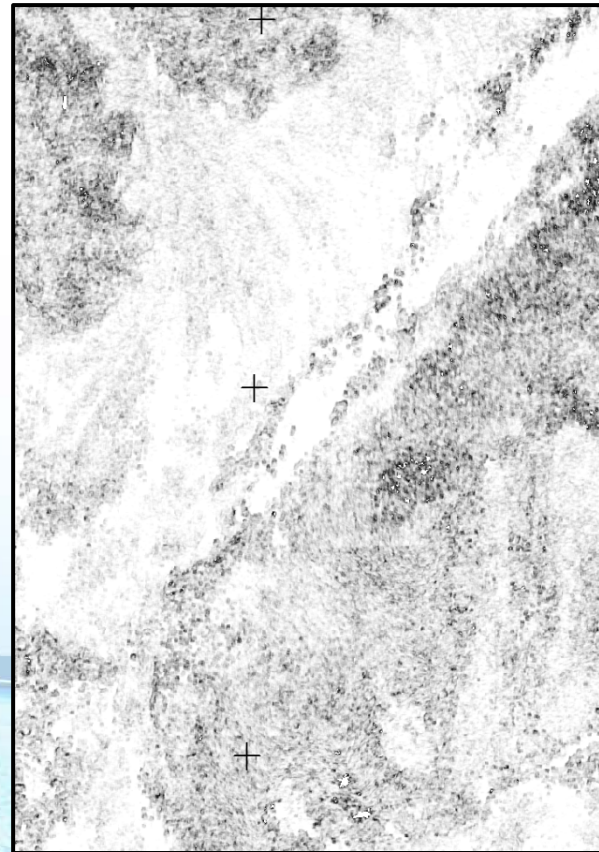
3.4 Result and Analysis

- The coherence correction results of **Airborne InSAR**
(Enlarged)

Range direction
↓



Before correction

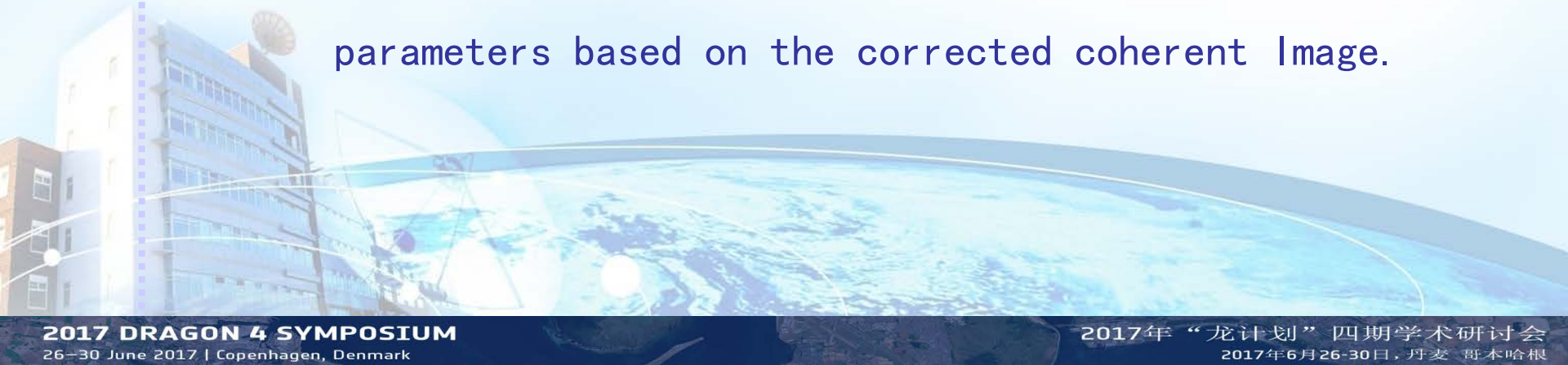


After correction

3.4 Result and Analysis

- Application of the Coherence Terrain Correction
 - Improve the ability of InSAR to classify and identify.
For example, the Interference Land Use (ILU) image:

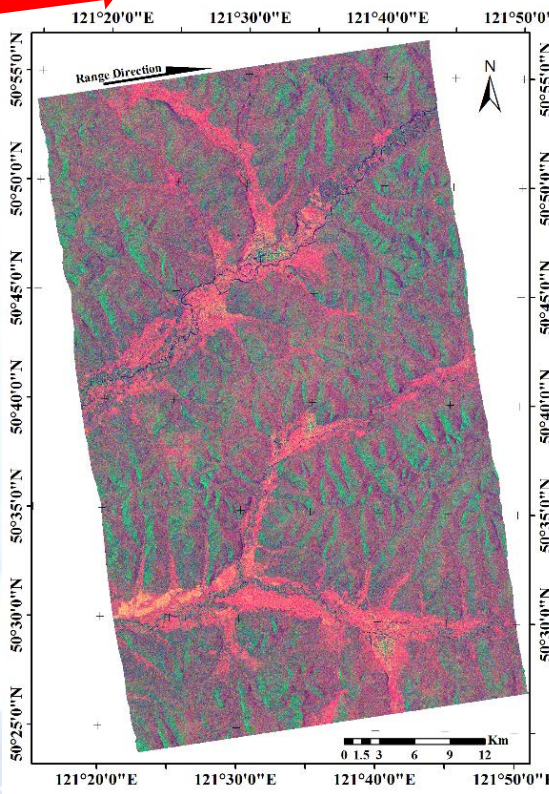
ILU image: ✓ R: InSAR Coherence
 ✓ G: Average intensity
 ✓ B: Intensity difference
 - Increasing the estimation accuracy of vegetation parameters based on the corrected coherent Image.



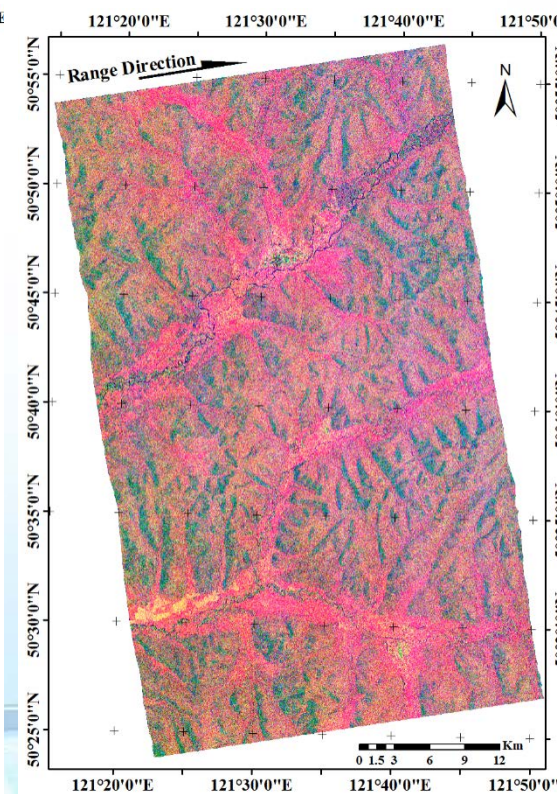
3.4 Result and Analysis

- The correction results of Space borne ILU image

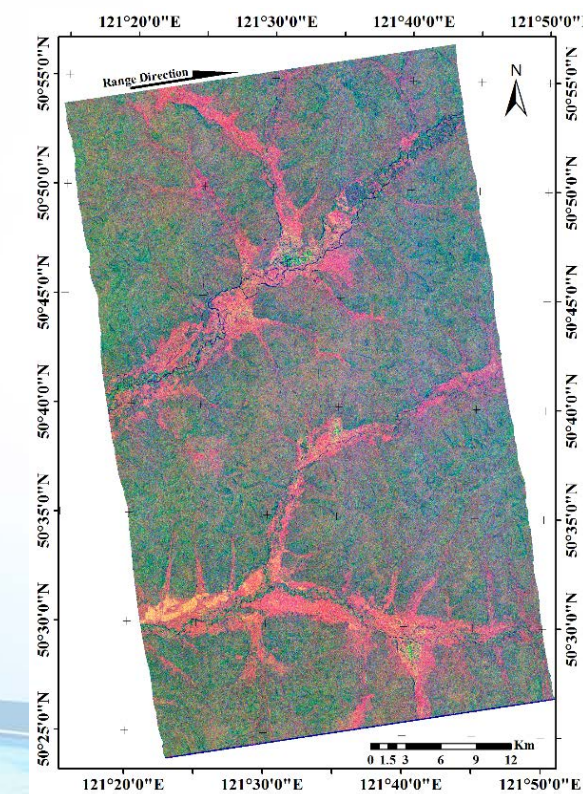
Range direction



Uncorrected intensity;
Uncorrected coherence.



Corrected intensity;
Uncorrected coherence.

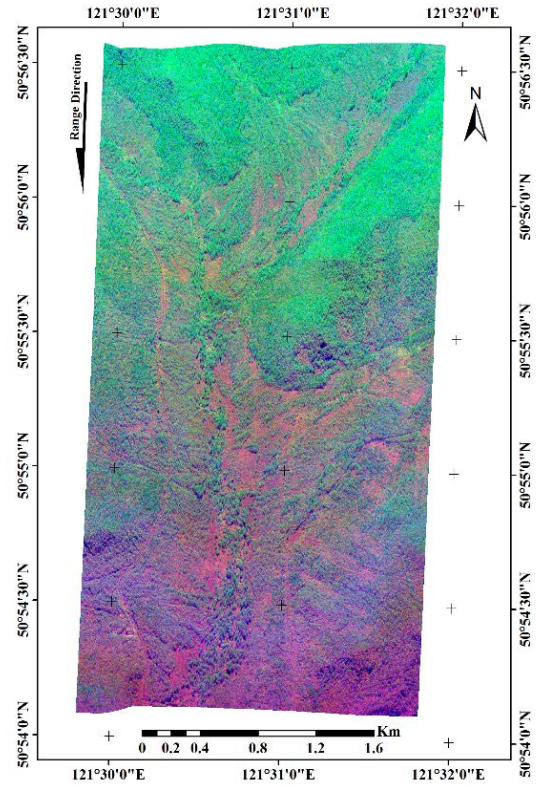


Corrected intensity;
Corrected coherence.

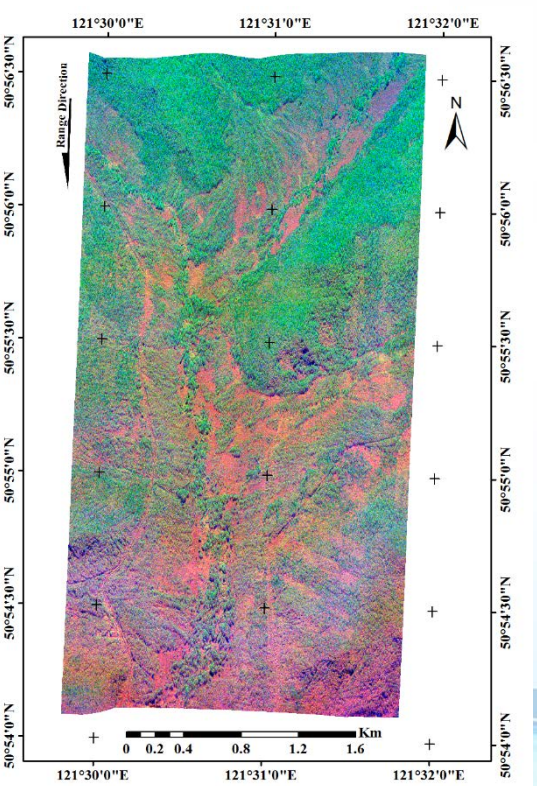
3.4 Result and Analysis

- The correction results of Airborne ILU image

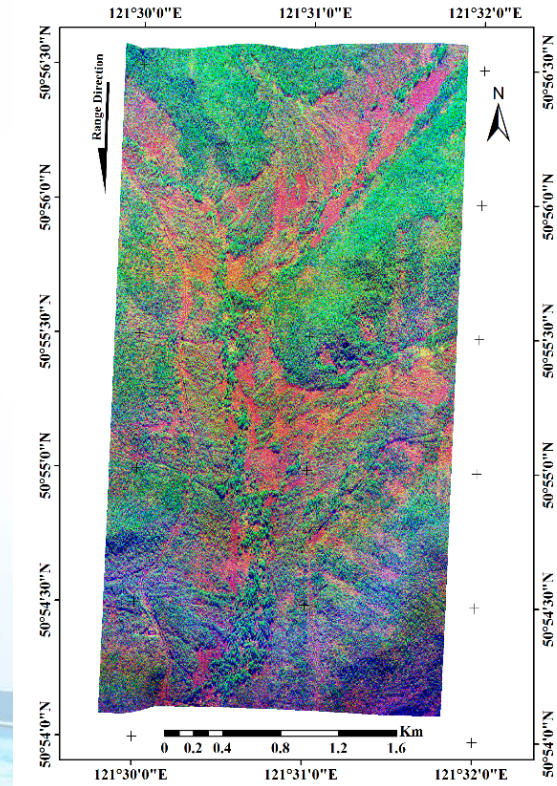
Range direction



Uncorrected intensity;
Uncorrected coherence.



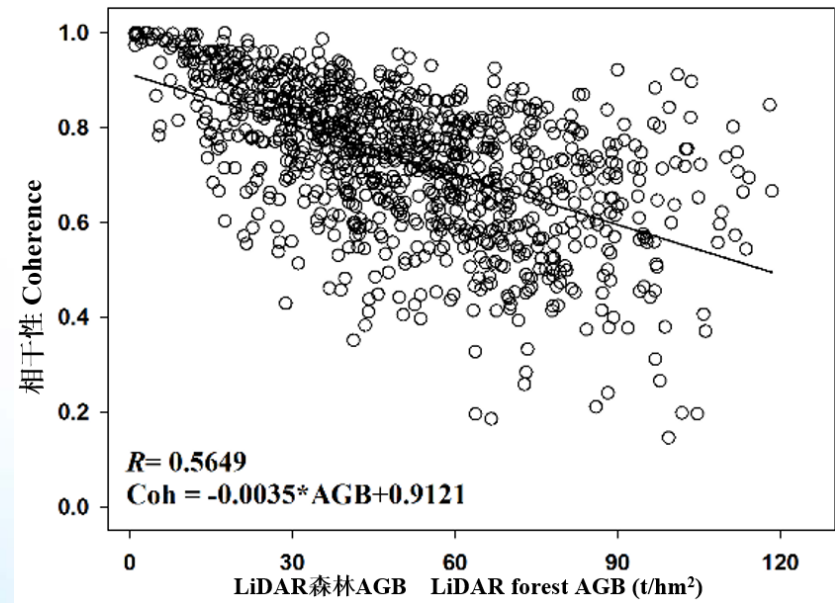
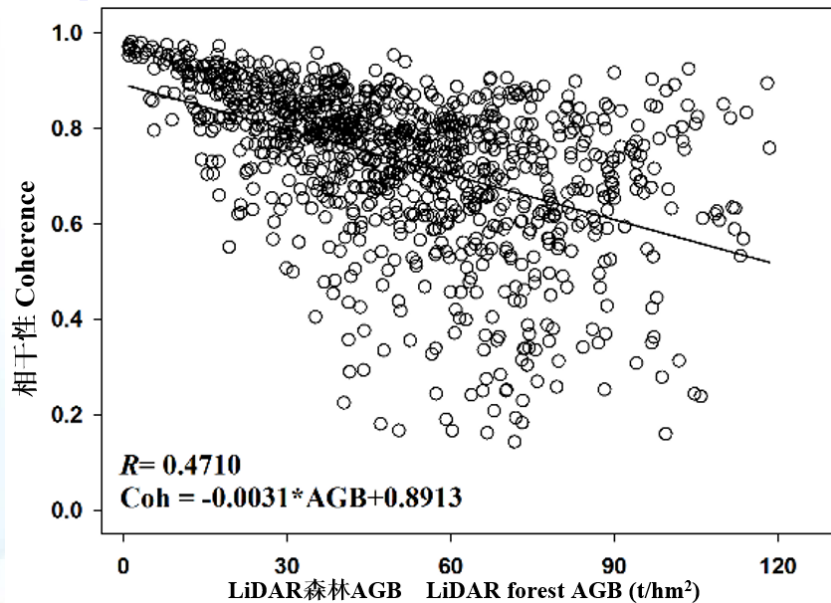
Corrected intensity;
Uncorrected coherence.



Corrected intensity;
Corrected coherence.

3.4 Result and Analysis

- The correlation between coherence (Space borne) and LiDAR forest AGB



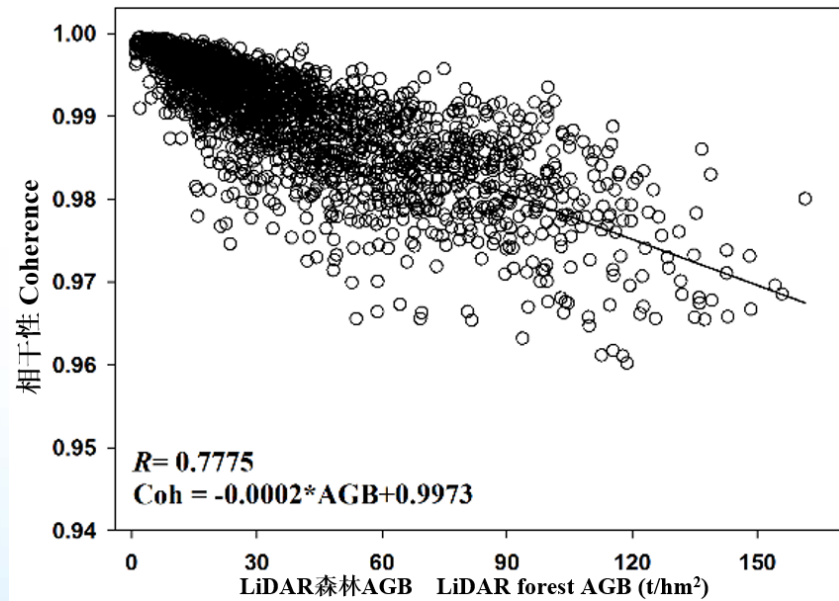
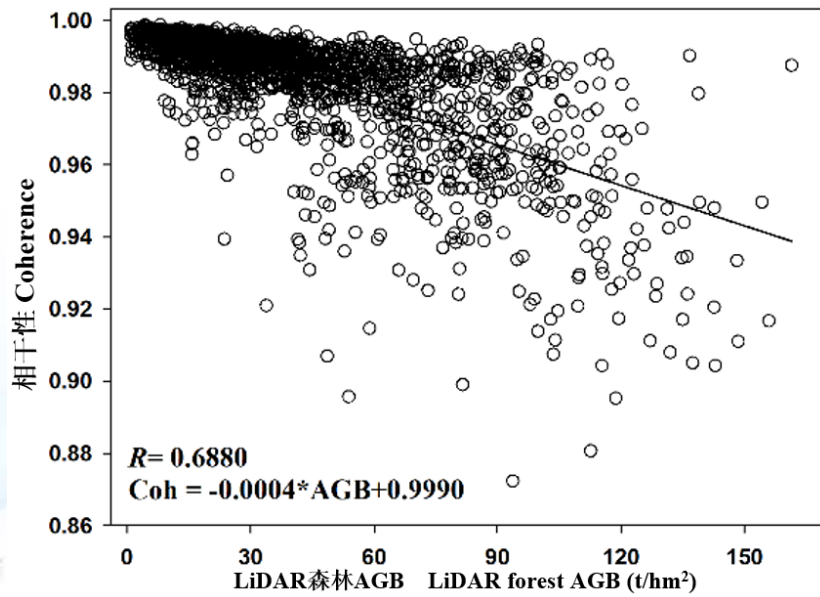
Before correction

+0.09

After correction

3.4 Result and Analysis

- The correlation between coherence (Airborne) and LiDAR forest AGB



Before correction

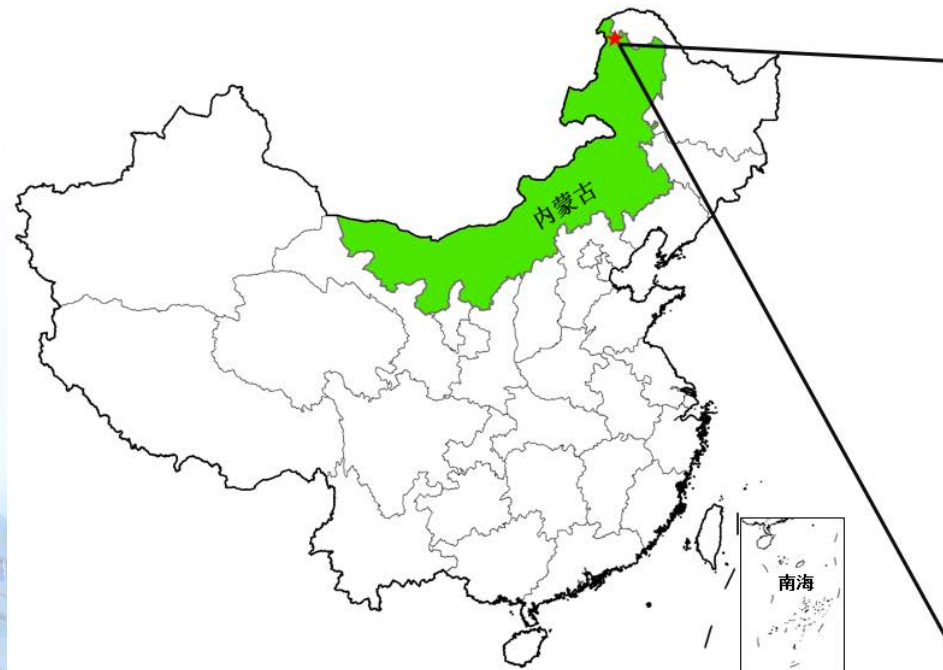
+0.09

After correction

1. Background
2. Three-Stage Terrain Correction Method For PolSAR
3. Terrain Correction Method For InSAR coherence
4. The combined estimation approach of Forest AGB
based on CASMSAR (X-InSAR, P-PoSAR)
5. Summary

4.1 Test Data

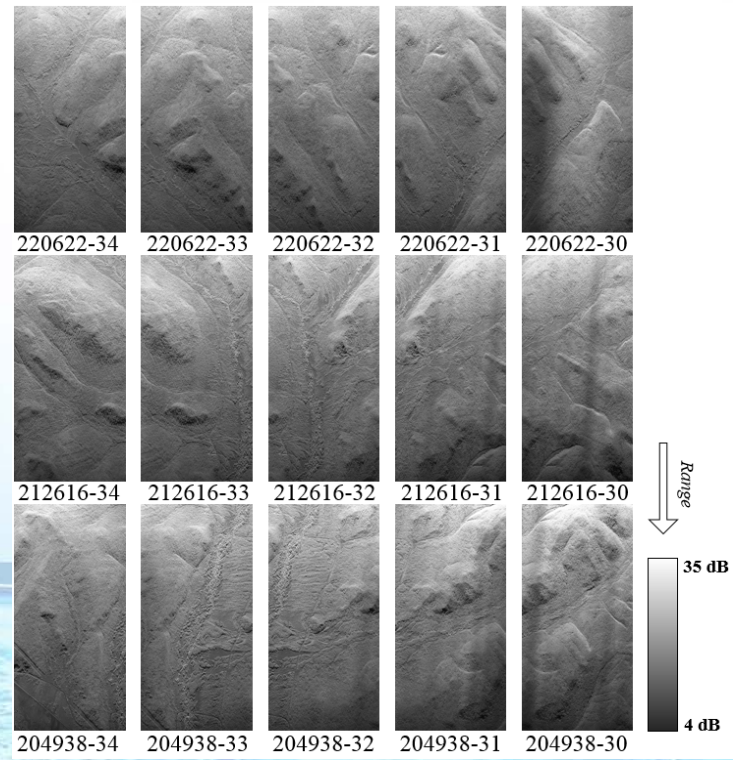
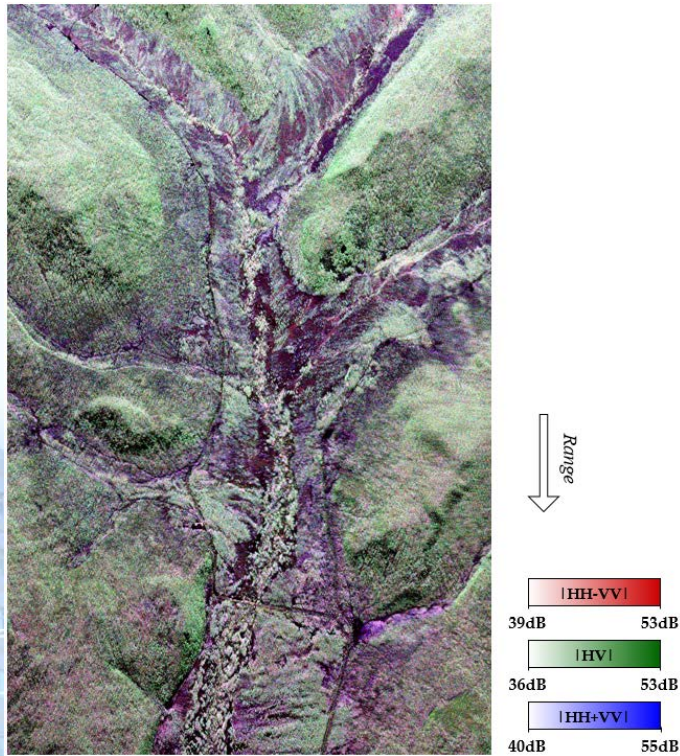
- DaXingAnLing test site in Inner Mongolia
 - China CASMSAR Multi-dimensional SAR System



X-InSAR (15 images)
 P-PolSAR(1 image)

4.1 Test Data

- China CASMSAR Multi-dimensional SAR System
 - P-band PolSAR
 - X-band HH InSAR

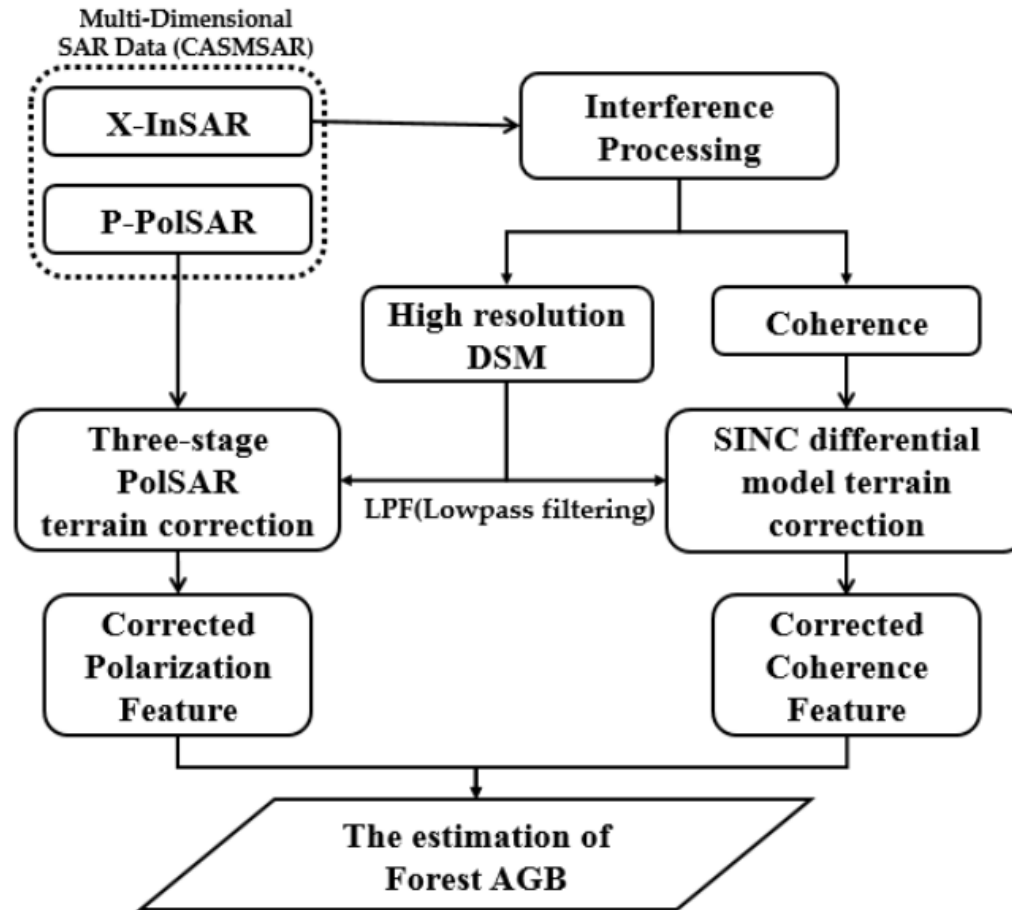


P-PolSAR PauliRGB

X-InSAR intensity image

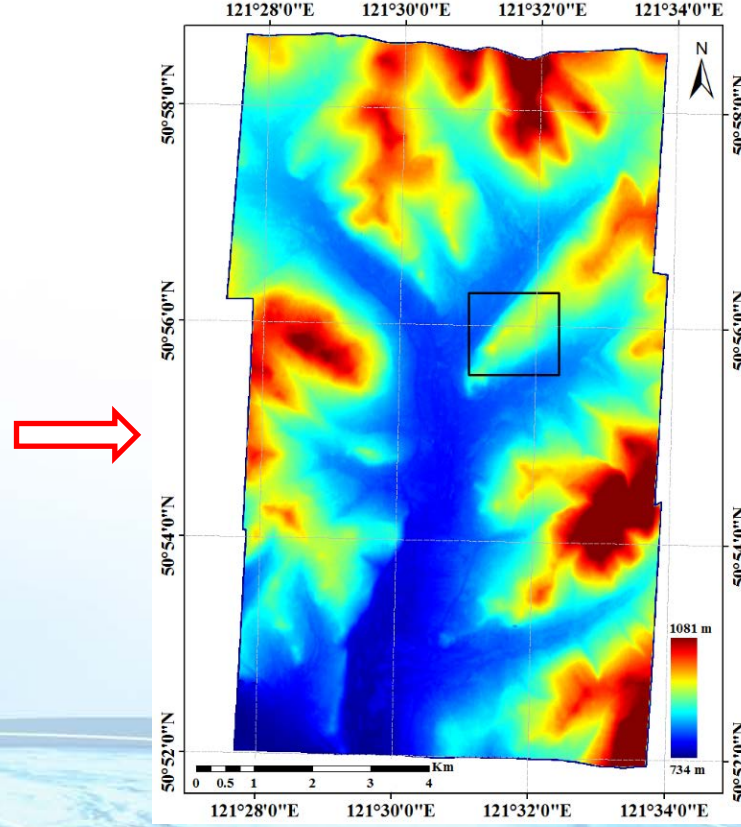
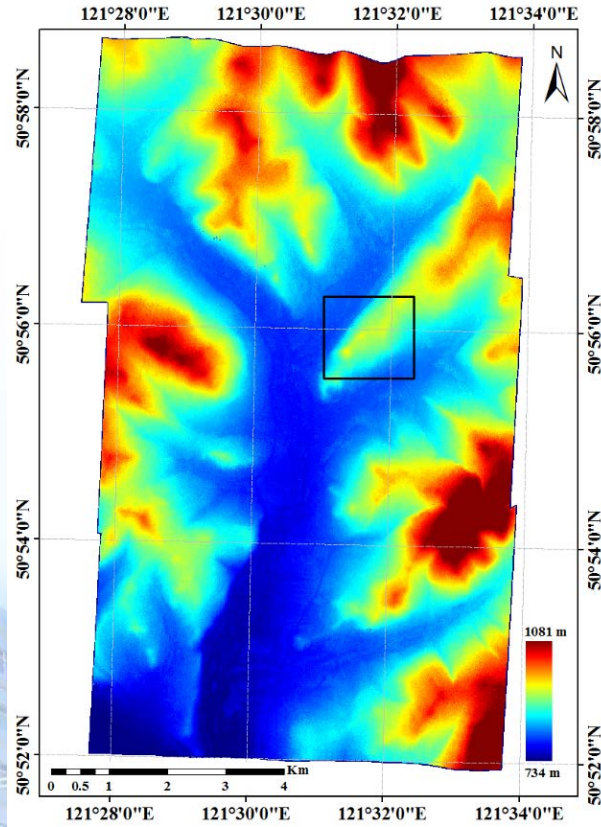
4.2 Methods

- Flow chart of combined estimation approach



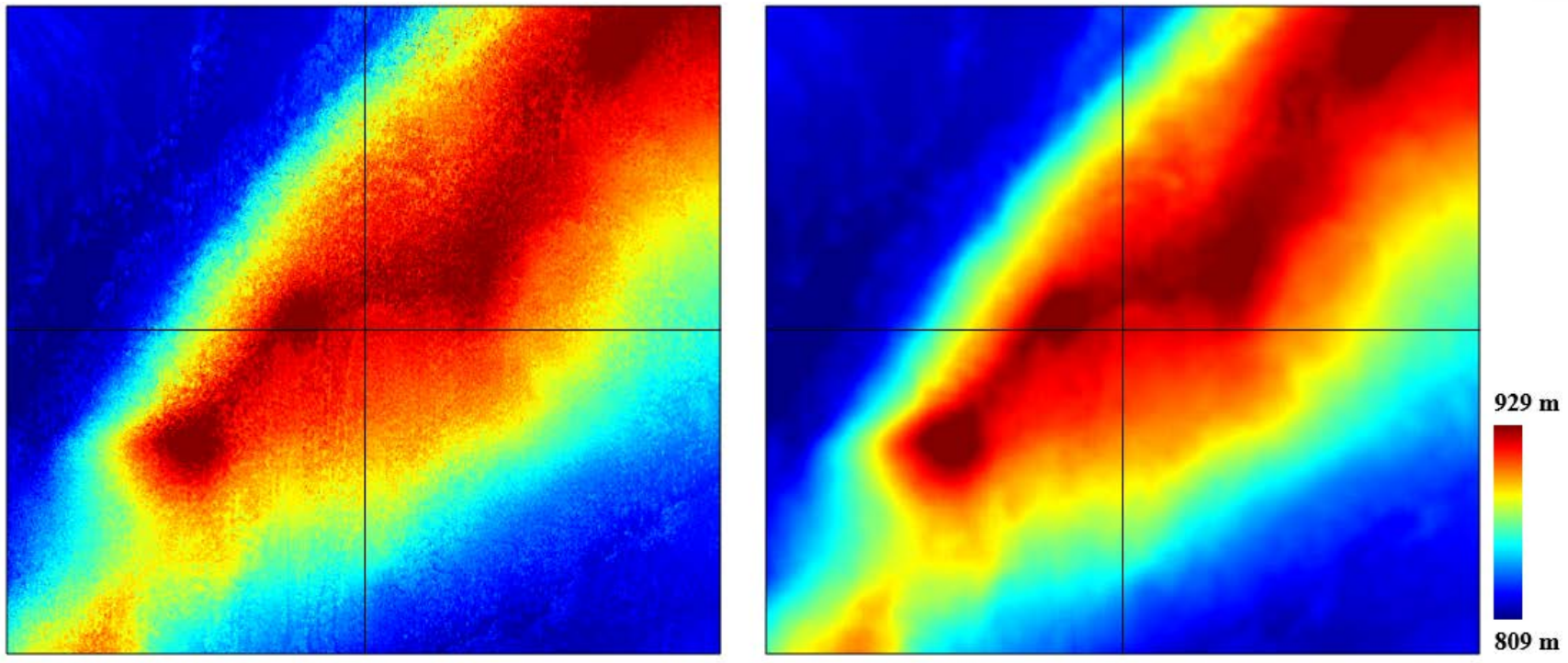
4.3 Result and Analysis

- X-InSAR interference processing result: DSM



4.3 Result and Analysis

- X-InSAR interference processing result: DSM
(Enlarged)



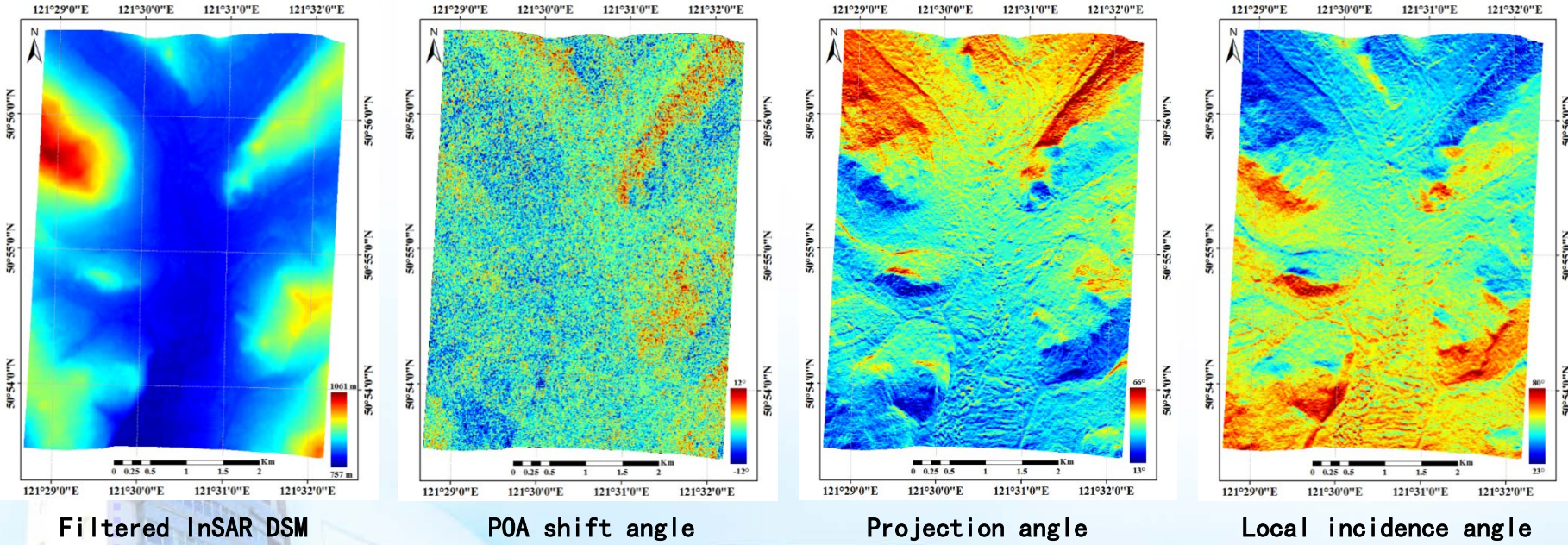
Original InSAR DSM



Lowpass filtered InSAR DSM

4.3 Result and Analysis

- Terrain correction results of P-PolSAR



4.3 Result and Analysis

- Terrain correction results of P-PolSAR

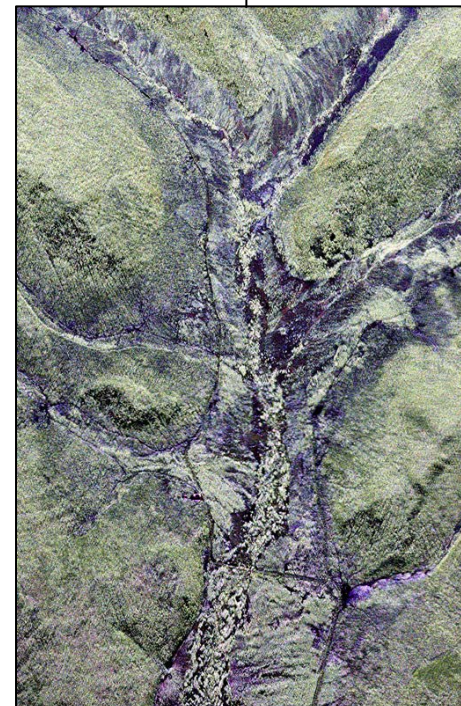
Step1: POAc



Step3: AVEc

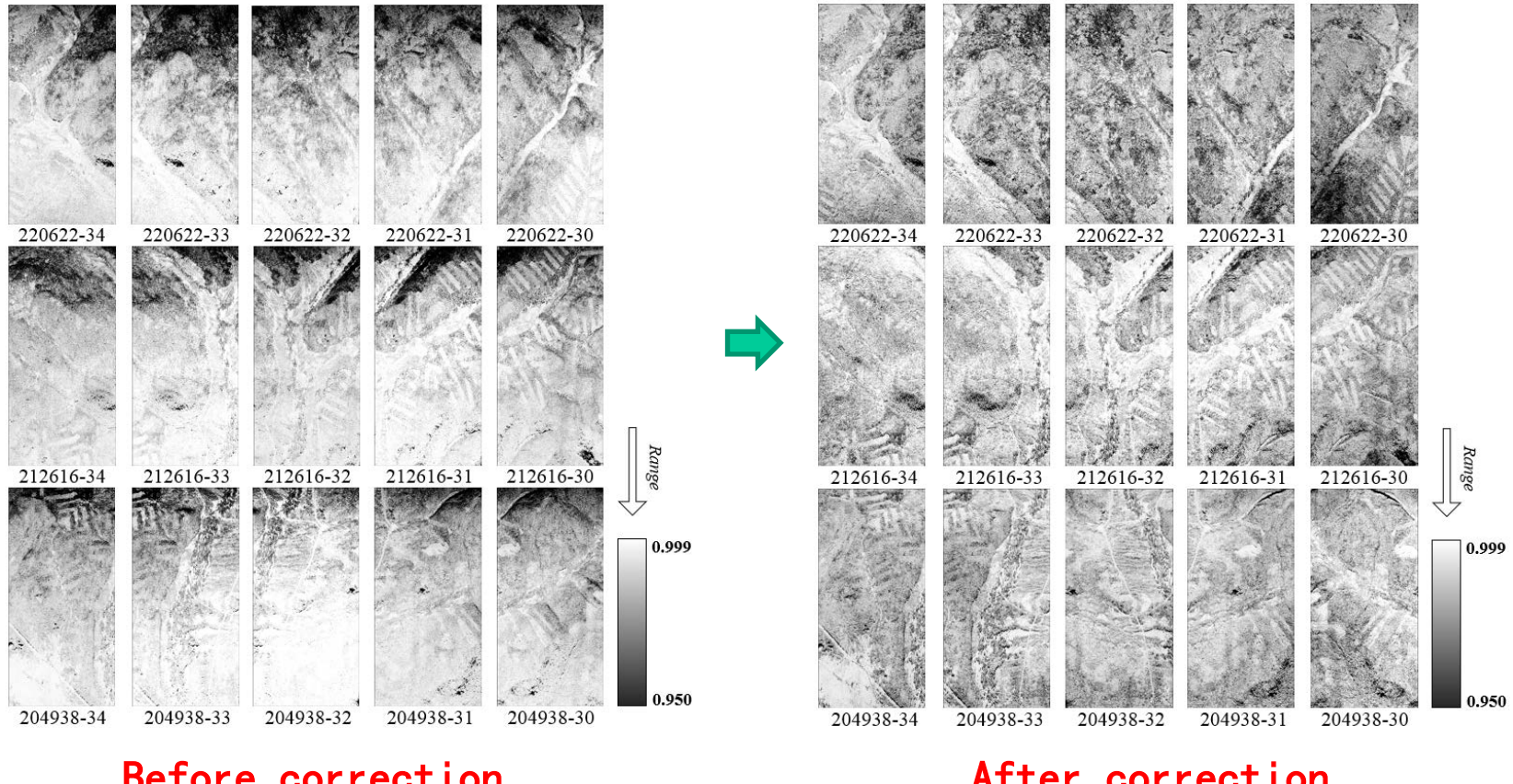


Step2: ESAc



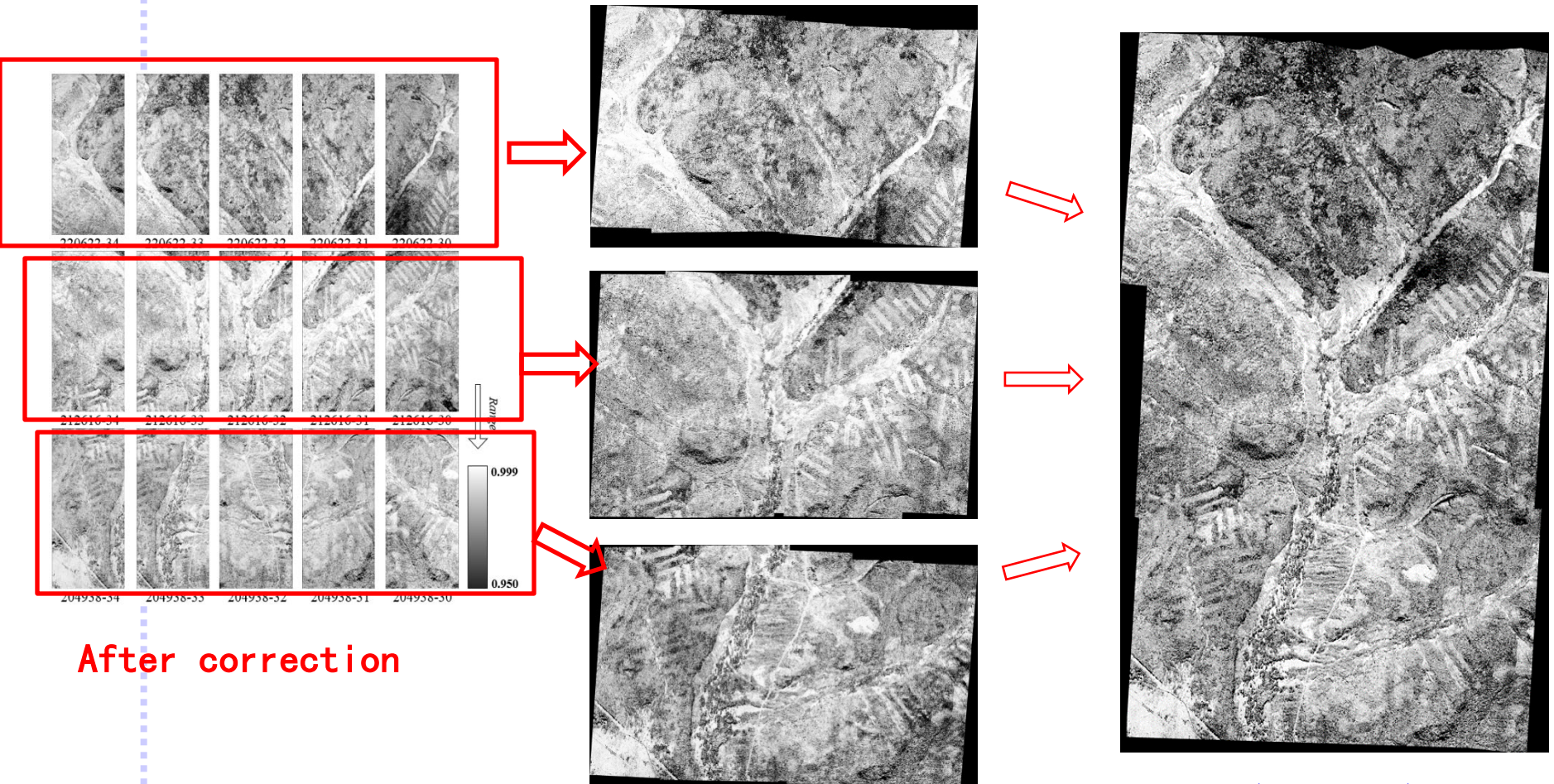
4.3 Result and Analysis

- Terrain correction results of X-InSAR coherence



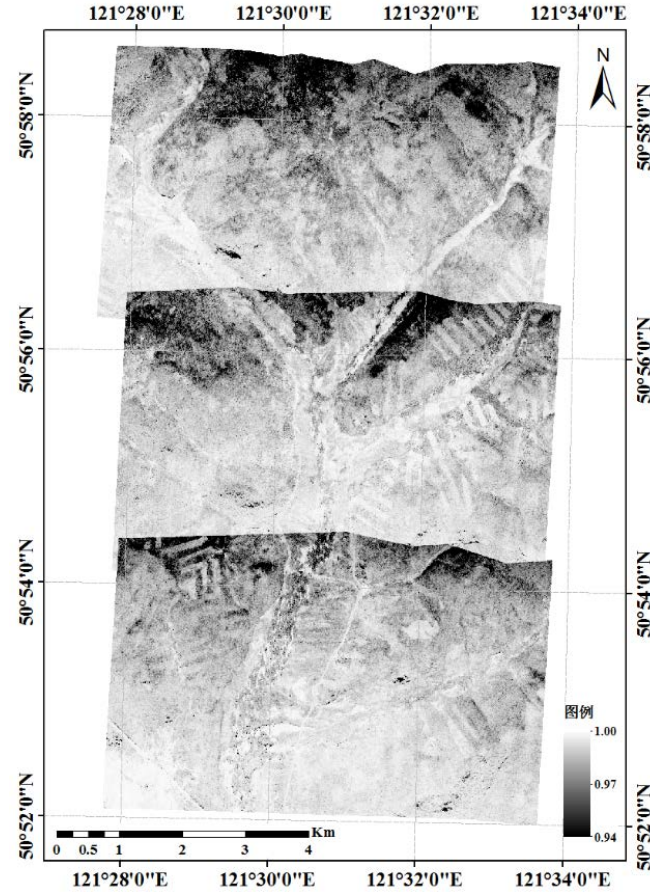
4.3 Result and Analysis

- Terrain correction results of X-InSAR coherence (Mosaic)

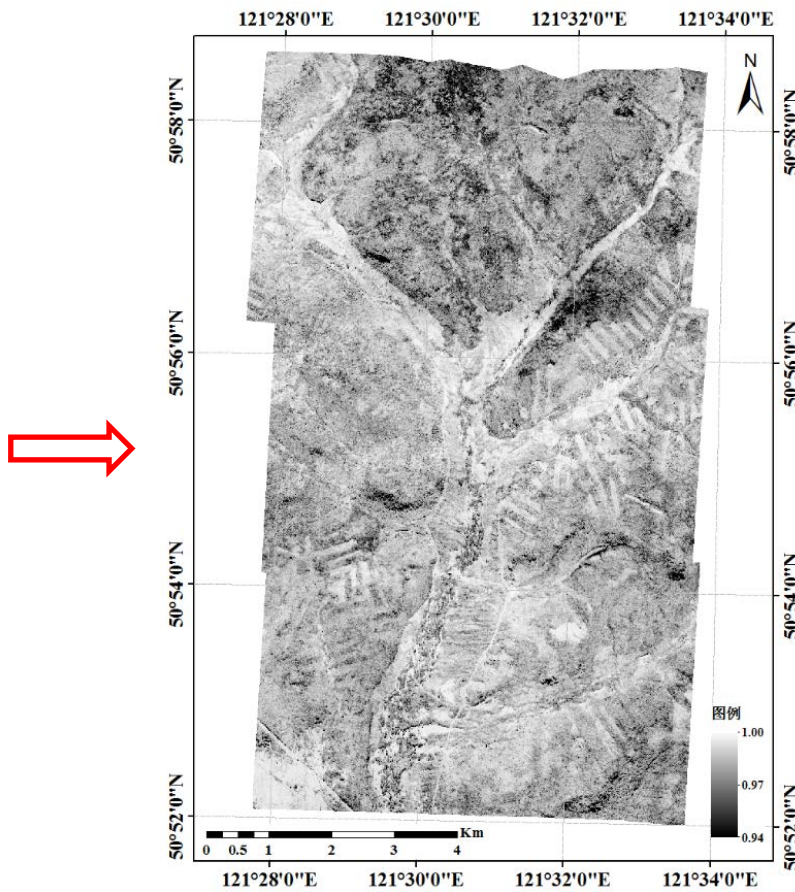


4.3 Result and Analysis

- Terrain correction results of X-InSAR coherence (Mosaic)



Before correction

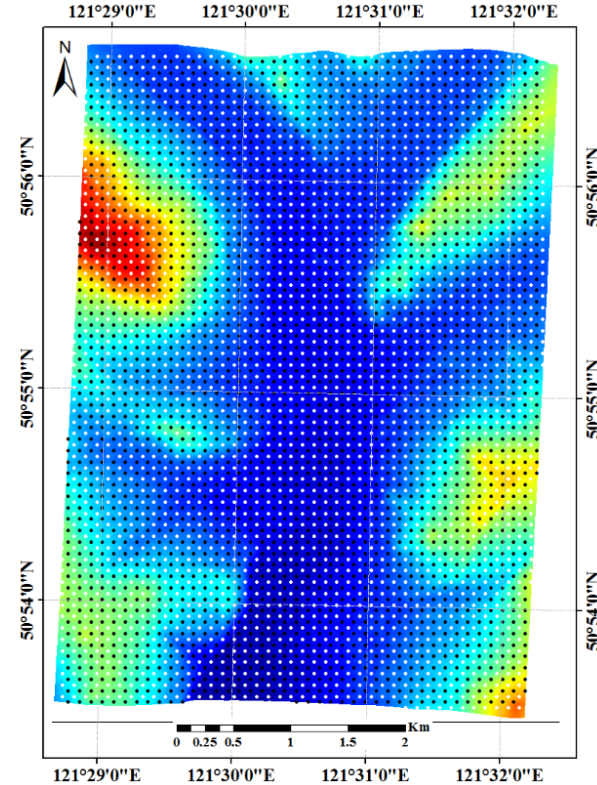
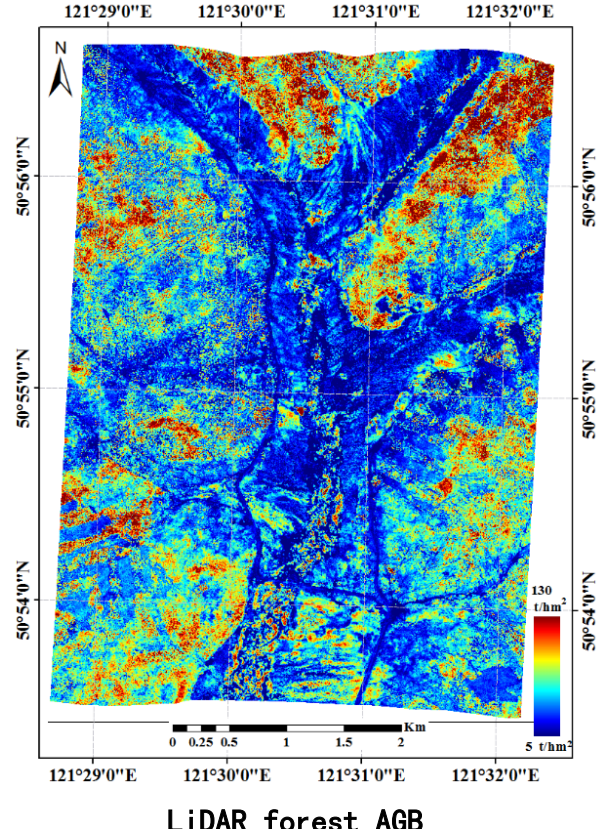


After correction

4.3 Result and Analysis

- Forest AGB combined estimation Modeling

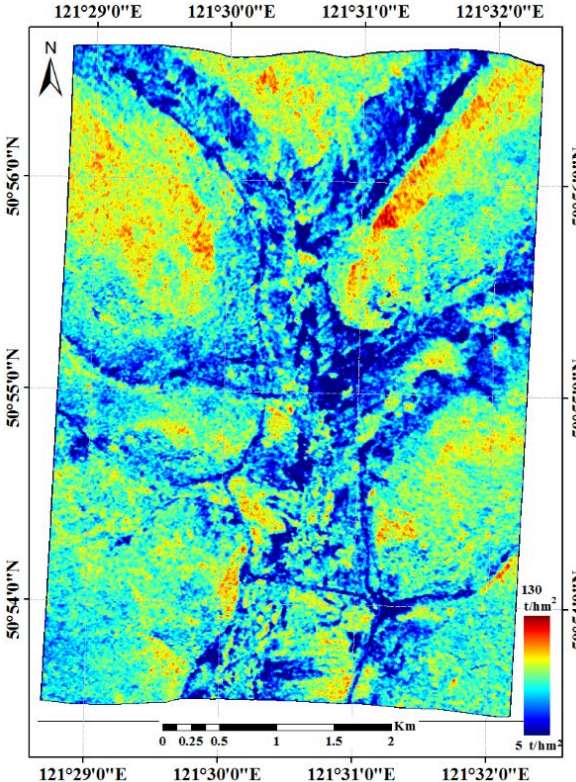
Model: $AGB = a + b \cdot HH + c \cdot HV + d \cdot VV + e \cdot Coherence$



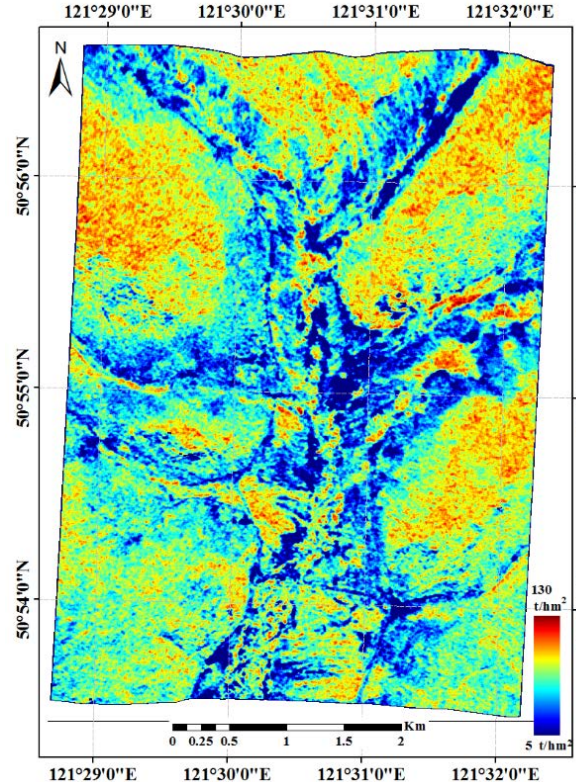
4.3 Result and Analysis

- Forest AGB estimation results: P-PoISAR

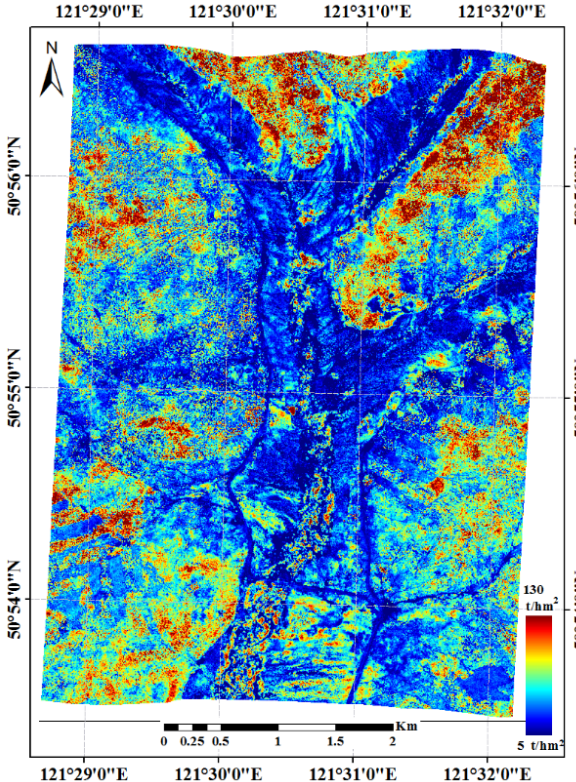
Model: $AGB = a + b \cdot HH + c \cdot HV + d \cdot VV$



Uncorrected P-PoISAR



Corrected P-PoISAR

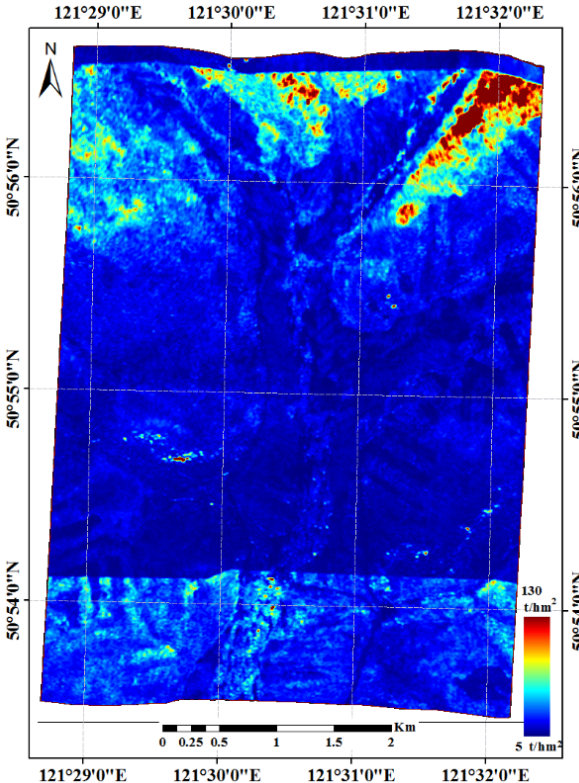


LiDAR forest AGB

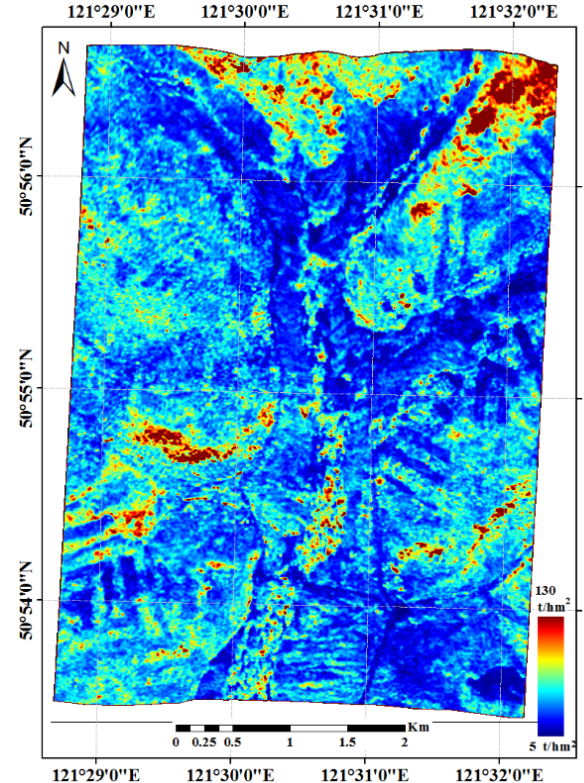
4.3 Result and Analysis

- Forest AGB estimation results: X-InSAR

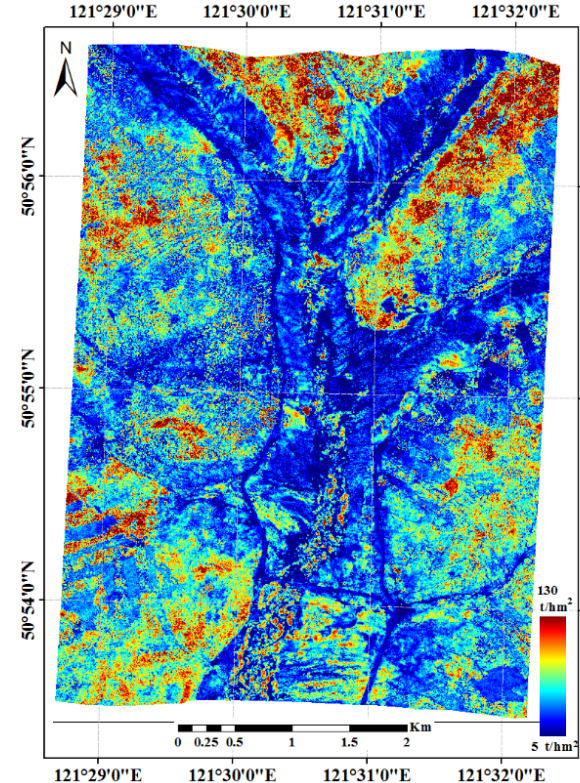
Model: $AGB = a + e \cdot \text{Coherence}$



Uncorrected coherence

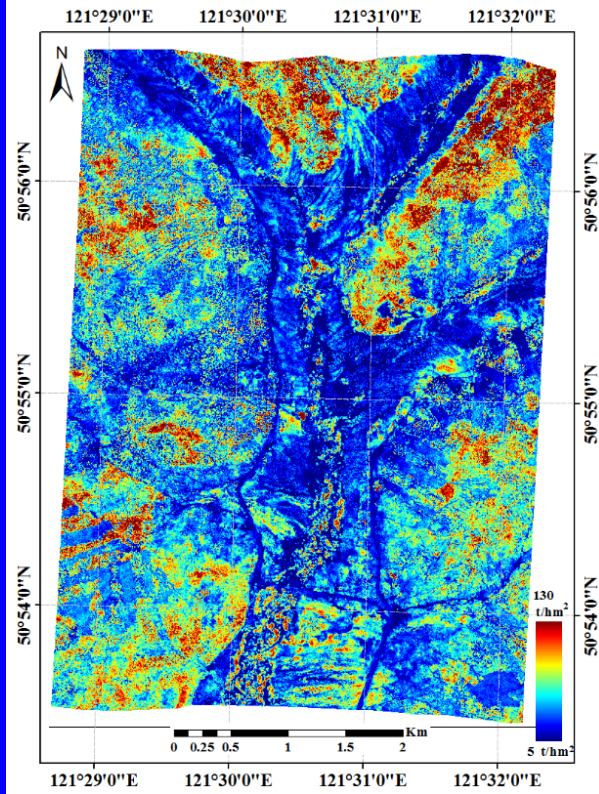
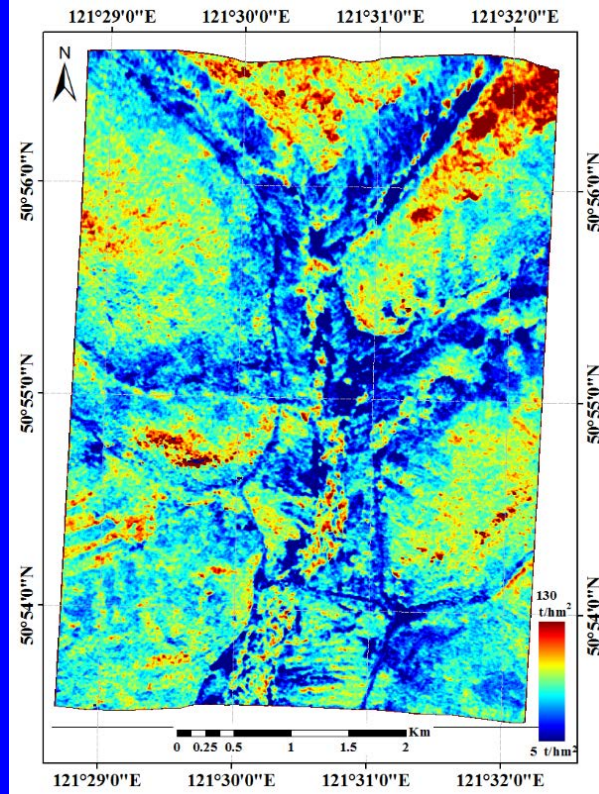
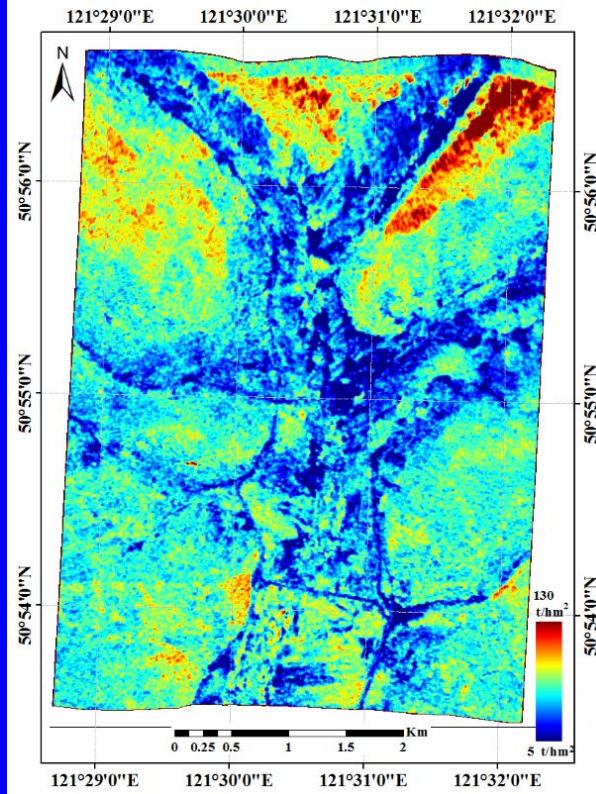


Corrected coherence



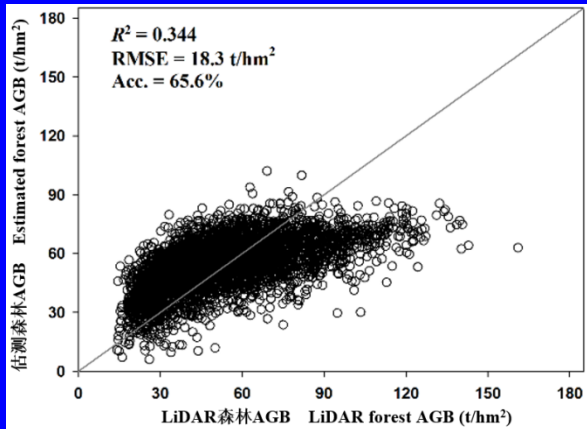
LiDAR forest AGB

- Forest AGB estimation results: P-PolSAR + X-InSAR
- Model: $AGB = a + b \cdot HH + c \cdot HV + d \cdot VV + e \cdot \text{Coherence}$

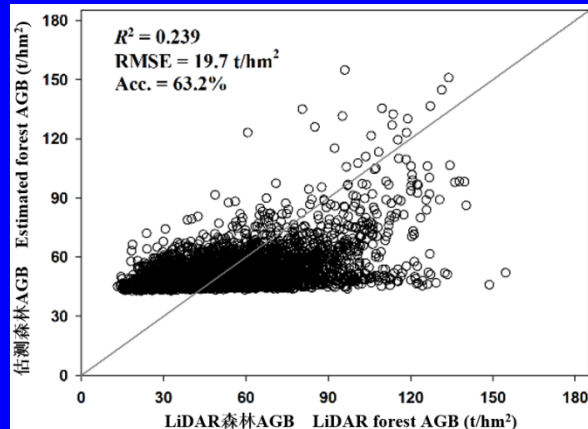


- Forest AGB estimation accuracy +3.7%

P-PoSAR

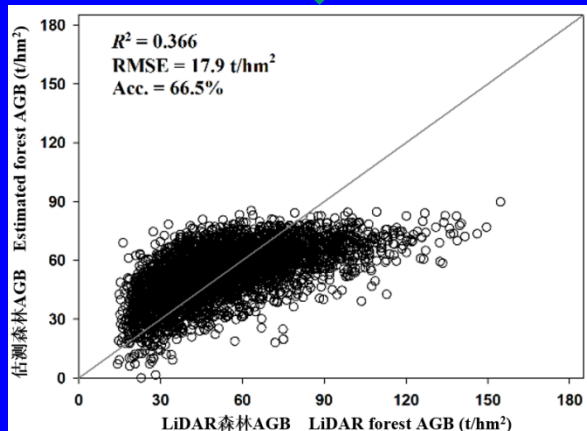
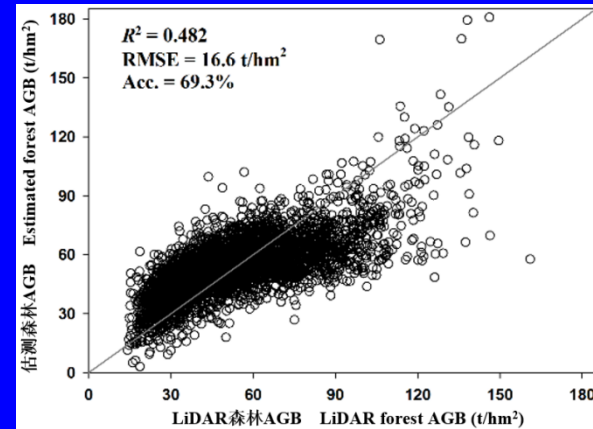


X-InSAR

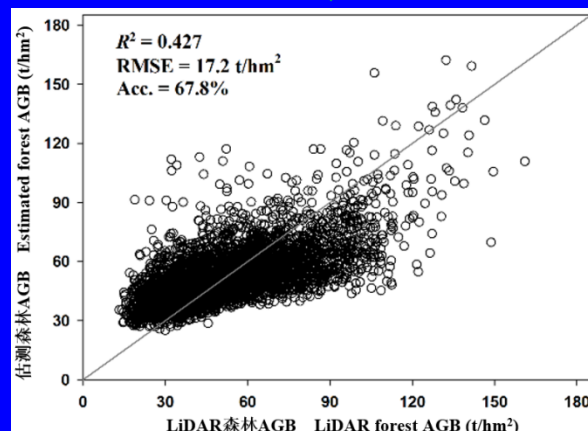


+6.1%

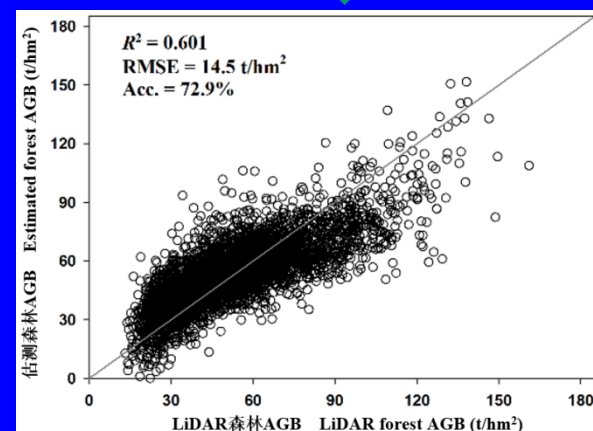
P-PoSAR+X-InSAR



↓ +0.09%



↓ +5.6%



↓ +3.6%

+6.4%

+5.1%

1. Background
2. Three-Stage Terrain Correction Method For PolSAR
3. Terrain Correction Method For InSAR coherence
4. The combined estimation approach of Forest AGB based on CASMSAR (X-InSAR, P-PoSAR)
5. Summary

5. Summary

Aiming at the terrain problem of multi-dimensional SAR data applied to forest AGB estimation:

- One three-stage terrain correction methods for PolSAR data was proposed
Three-stage method has advanced features in systematic comprehensive correction and self-adaptive parameter settings. And it is suitable for PolSAR matrix data.
- SINC differential correction method for InSAR coherence was developed
It can effectively improve the image quality of ILU image & improve the correlation between coherence and forest AGB.
- Combined estimation approach for forest AGB based on X-band InSAR and P-band PolSAR data.
It shows that the terrain effect of multi-dimensional SAR data can be effectively removed by proposed method. And the accuracy of forest AGB estimation can be improved.

Thank you for your attentions !